

o

# Numerical Modelling of Tides in Hudson Strait and Ungava Bay

P.C.P. Chandler, S. de Margerie, and J.D. Covill

*Published by:*  
Atlantic Region  
Canadian Hydrographic Service  
Ocean Science and Surveys, Atlantic  
Department of Fisheries and Oceans

Bedford Institute of Oceanography  
P.O. Box 1006  
Dartmouth, Nova Scotia B2Y 4A2

August 1985

11  
**Canadian Contractor Report of  
Hydrography and Ocean Sciences  
No. 13**

Spec Coll.  
DOCUMENTS

LIBRARY  
BEDFORD INSTITUTE  
OF OCEANOGRAPHY  
JAN 7 1986  
BIBLIOTHÈQUE  
INSTITUT Océanographique  
DE BEDFORD

PLEASE DO NOT  
REMOVE FROM  
LIBRARY

## **Canadian Contractor Report of Hydrography and Ocean Sciences**

These reports are unedited final reports from scientific and technical projects contracted by the Ocean Science and Surveys (OSS) sector of the Department of Fisheries and Oceans.

The contents of the reports are the responsibility of the contractor and do not necessarily reflect the official policies of the Department of Fisheries and Oceans.

If warranted, Contractor Reports may be rewritten for other publications series of the Department, or for publication outside the government.

Contractor Reports are produced regionally but are numbered and indexed nationally. Requests for individual reports will be fulfilled by the issuing establishment listed on the front cover and title page. Out of stock reports will be supplied for a fee by commercial agents.

Regional and headquarters establishments of Ocean Science and Surveys ceased publication of their various report series as of December 1981. A complete listing of these publications and the last number issued under each title are published in the *Canadian Journal of Fisheries and Aquatic Sciences*, Volume 38: Index to Publications 1981. The current series began with Report Number 1 in January 1982.

## **Rapport canadien des entrepreneurs sur l'hydrographie et les sciences océaniques**

Cette série se compose des rapports non publiés réalisés dans le cadre des projets scientifiques et techniques par des entrepreneurs travaillant pour le service des Sciences et Levés océaniques (SLO) du ministère des Pêches et des Océans.

Le contenu des rapports traduit les opinions de l'entrepreneur et ne reflète pas nécessairement la politique officielle du ministère des Pêches et des Océans.

Le cas échéant, certains rapports peuvent être rédigés à nouveau de façon à être publiés dans une autre série du Ministère, ou à l'extérieur du Gouvernement.

Les rapports des entrepreneurs sont produits à l'échelon régional mais sont numérotés et placés dans l'index à l'échelon national. Les demandes de rapports seront satisfaites par l'établissement auteur dont le nom figure sur la couverture et la page de titre. Les rapports épuisés seront fournis contre rétribution par des agents commerciaux.

Les établissements des Sciences et Levés océaniques dans les régions et à l'administration centrale ont cessé de publier leurs diverses séries de rapports depuis décembre 1981. Vous trouverez dans l'index des publications du volume 38 du *Journal canadien des sciences halieutiques et aquatiques*, la liste de ces publications ainsi que le dernier numéro paru dans chaque catégorie. La nouvelle série a commencé avec la publication du Rapport n° 1 en janvier 1982.

Canadian Contractor Report of  
Hydrography and Ocean Sciences No. 13

August 1985

NUMERICAL MODELLING OF TIDES IN HUDSON STRAIT AND UNGAVA BAY\*

by

P.C.P. Chandler<sup>1</sup>, S. de Margerie<sup>2</sup>, and J.D. Covill<sup>1</sup>

Published by:  
Atlantic Region  
Canadian Hydrographic Service  
Ocean Science and Surveys, Atlantic

Bedford Institute of Oceanography  
P.O. Box 1006  
Dartmouth, N.S.  
B2Y 4A2

<sup>1</sup> Martec Limited, 5670 Spring Garden Road, Halifax, Nova Scotia.

<sup>2</sup> ASA Consulting Ltd., P.O. Box 2025, Dartmouth, Nova Scotia.

\* Prepared under contract no. 08SC.FP901-4-R533  
for the Canadian Hydrographic Service.

ACKNOWLEDGEMENTS

The scientific authority, Mr. Stephen Grant, P.Eng., and his staff in the Tidal Division (Atlantic Region of Canadian Hydrographic Service) deserve recognition for their valuable assistance. The contribution of Dr. David Greenberg, Atlantic Oceanographic Laboratory, to the numerical modelling aspect of the project was a definite asset and greatly appreciated.

©Minister of Supply and Services Canada 1985  
Cat. No. FS 97-17/13E ISSN 0711-6748

Correct citation for this publication:

Chandler, P.C.P., de Margerie, S., and Covill, J.D. 1985. Numerical modelling of tides in Hudson Strait and Ungava Bay. Can. Contract. Rep. Hydrogr. Ocean Sci. No. 13: vii + 60 p.

ABSTRACT

Chandler, P.C.P., de Margerie, S., and Covill, J.D. 1985. Numerical modelling of tides in Hudson Strait and Ungava Bay. Can. Contract. Rep. Hydrogr. Ocean Sci. No. 13: vii + 60 p.

A two-dimensional numerical model was applied to the Hudson Strait and Ungava Bay region to simulate the barotropic tidal circulation. Four fundamental frequencies, the  $M_2$ ,  $S_2$ ,  $N_2$  and  $K_1$ , were modelled and calibrated to observed tidal data in the study area. The non-linear interaction of these four constituents was examined by conducting a tidal analysis on the results of a 24 day simulation modelling of all four components simultaneously.

Current vector plots of the  $M_2$  tide at intervals of one hour were produced, using high water at Diana Bay ( $61^\circ\text{N}$ ,  $70^\circ\text{W}$ ) as a reference. Cotidal charts of the model area for the  $M_2$ ,  $S_2$ ,  $N_2$ , and  $K_1$  constituents were generated and compared to tidal information derived from previous analytical and numerical studies.

The general circulation of the study area was well represented by the numerical model. Agreement between observed and modelled characteristics of the  $M_2$  tide is generally better than  $\pm 4\%$  or  $\pm 8$  cm for amplitude and  $13^\circ$  (26 minutes) for phase. The absolute error for the other modelled constituents is of a similar order.

RESUME

Chandler, P.C.P., de Margerie, S., and Covill, J.D. 1985. Numerical modelling of tides in Hudson Strait and Ungava Bay. Can. Contract. Rep. Hydrogr. Ocean Sci. No. 13: vii + 60 p.

Un modèle numérique bi-dimensionnel a été utilisé dans le détroit d'Hudson et la région de la baie d'Ungava pour simuler les courants de marée barotropiques. Quatre fréquences fondamentales ont été modélisées, soit  $M_2$ ,  $S_2$ ,  $N_2$  et  $K_1$ . Ces constituantes ont été calibrées à partir des données marégraphiques de la région étudiée. Les interactions non-linéaires de ces quatre constituantes ont été analysées en simulant leur comportement simultanément pendant une période de vingt-quatre jours.

Les courants sont représentés à intervalle d'une heure par des cartes de vecteurs utilisant l'heure de la marée haute à Diana Bay ( $61^\circ\text{N}$ ,  $70^\circ\text{W}$ ) comme point de référence. Les cartes cotidiales des constituantes  $M_2$ ,  $S_2$ ,  $N_2$  et  $K_1$  obtenues à l'aide du modèle ont été comparées aux informations tirées d'études analytiques et numériques précédentes.

Le modèle numérique reproduit adéquatement la circulation générale de la zone étudiée. Les caractéristiques simulées et observées de la constituante  $M_2$  se comparent en deça d'une erreur de 4% ( $\pm 8\text{cm}$ ) pour l'amplitude et de  $13^\circ$  (26 min) pour la phase. L'erreur absolue est du même ordre de grandeur pour les autres constituantes.

TABLE OF CONTENTS

ACKNOWLEDGEMENTS .....	ii
ABSTRACT - RESUME .....	iii
TABLE OF CONTENTS .....	v
LIST OF FIGURES .....	vi
LIST OF TABLES .....	vii
1. INTRODUCTION .....	1
2. BACKGROUND TIDAL INFORMATION .....	4
3. THE BAROTROPIC TIDAL MODEL .....	12
3.1 Digitization of the Model Bathymetry .....	12
3.2 Model Boundary Conditions and Calibration .....	14
3.3 Model Implementation for the Hudson Strait/Ungava Bay Study Area .....	18
3.4 Simulation of the Combined $M_2$ , $S_2$ , $N_2$ and $K_1$ Tidal Regimes .....	20
4. MODEL RESULTS .....	21
4.1 Tidal Elevations .....	21
4.2 Tidal Currents .....	29
4.3 Tidal Ellipses .....	43
4.4 Sensitivity of Model Bathymetry .....	52
4.5 Discussion .....	52
5. REFERENCES .....	54
APPENDIX I - Comparison of Observed and Modelled Tides in Hudson Strait and Ungava Bay .....	56

LIST OF FIGURES

FIGURE 1.	Location Map of Study Area .....	2
FIGURE 2.	Locations of Tidal Information Stations .....	5
FIGURE 3.	Previous Cotidal Charts for the $M_2$ Tide .....	10
FIGURE 4.	Model Area .....	13
FIGURE 5.	Bathymetry of the Model Area .....	15
FIGURE 6.	Cotidal Chart for the $M_2$ Tide in the Model Area .....	24
FIGURE 7.	Cotidal Chart for the $S_2$ Tide in the Model Area .....	25
FIGURE 8.	Cotidal Chart for the $N_2$ Tide in the Model Area .....	26
FIGURE 9.	Cotidal Chart for the $K_1$ Tide in the Model Area .....	27
FIGURE 10.	Tidal Currents at High Water, Diana Bay .....	30
FIGURE 11.	Tidal Currents One Hour After High Water at Diana Bay .....	31
FIGURE 12.	Tidal Currents Two Hours After High Water at Diana Bay .....	32
FIGURE 13.	Tidal Currents Three Hours After High Water at Diana Bay .....	33
FIGURE 14.	Tidal Currents Four Hours After High Water at Diana Bay .....	34
FIGURE 15.	Tidal Currents Five Hours After High Water at Diana Bay .....	35
FIGURE 16.	Tidal Currents Six Hours After High Water at Diana Bay .....	36
FIGURE 17.	Tidal Currents Seven Hours After High Water at Diana Bay .....	37
FIGURE 18.	Tidal Currents Eight Hours After High Water at Diana Bay .....	38
FIGURE 19.	Tidal Currents Nine Hours After High Water at Diana Bay .....	39



LIST OF FIGURES (Continued)

FIGURE 20.	Tidal Currents Ten Hours After High Water at Diana Bay .....	40
FIGURE 21.	Tidal Currents 11 Hours After High Water at Diana Bay .....	41
FIGURE 22.	Tidal Ellipses for the $M_2$ Tide in the Model Area .....	48
FIGURE 23.	Tidal Ellipses for the $S_2$ Tide in the Model Area .....	49
FIGURE 24.	Tidal Ellipses for the $N_2$ Tide in the Model Area .....	50
FIGURE 25.	Tidal Ellipses for the $K_1$ Tide in the Model Area .....	51

LIST OF TABLES

TABLE 1.	Tidal Information at Stations Within the Model Boundary Determined from Observed Tidal Data .....	6
TABLE 2.	Model Boundary Conditions .....	17
TABLE 3.	Comparison of Amplitudes of Observed and Modelled Tides ...	22
TABLE 4.	Comparison of Phases of Observed and Modelled Tides .....	23
TABLE 5.	Comparison of Predicted and Observed Tidal Flows .....	44



## 1. INTRODUCTION

There is a growing interest in Canada's arctic waterways related to marine traffic navigation, natural resources exploration, and in the harnessing of tidal energy in Ungava Bay. To further our knowledge of water levels and currents in this region the Canadian Hydrographic Service has implemented a multi-dimensional project including field work, analytical and numerical studies. One aspect of this project is the development of a numerical model to provide information on the tidal elevations and currents in the Hudson Strait/Ungava Bay region shown in Figure 1.

Accurate determination of the tidal circulation in the Hudson Strait/Ungava Bay system is of significant importance since tides are responsible for the major part of the currents and sea surface elevation changes in this region. Tidal currents are of interest to navigators and also strongly affect the mixing and transport of water masses which support the northern ecosystem. Knowledge of the tidal range is necessary in planning harbour facilities, and in addition the large tides at the head of Ungava Bay make this a promising area for tidal power generation.

A two year study to numerically describe the tidal regime was carried out by Martec Limited under contract to the Canadian Hydrographic Service (File No. 10SC.FP901-3-R062 and 08SC.FP901-4-R533) (Martec, 1984a). Using a modified version of the Martec/AOL (Atlantic Oceanographic Laboratory) two-dimensional numerical model the barotropic circulation within the study area was simulated and compared with existing tidal data. The four main tidal constituents were modelled: the  $M_2$  (the principal lunar semidiurnal constituent), the  $S_2$  (the principal solar semidiurnal constituent), the  $N_2$  (the lunar elliptic semidiurnal constituent), and the  $K_1$  (the principal lunisolar diurnal constituent). Scale analysis revealed that the non-linear interaction between these constituents would be significant at the eastern end of

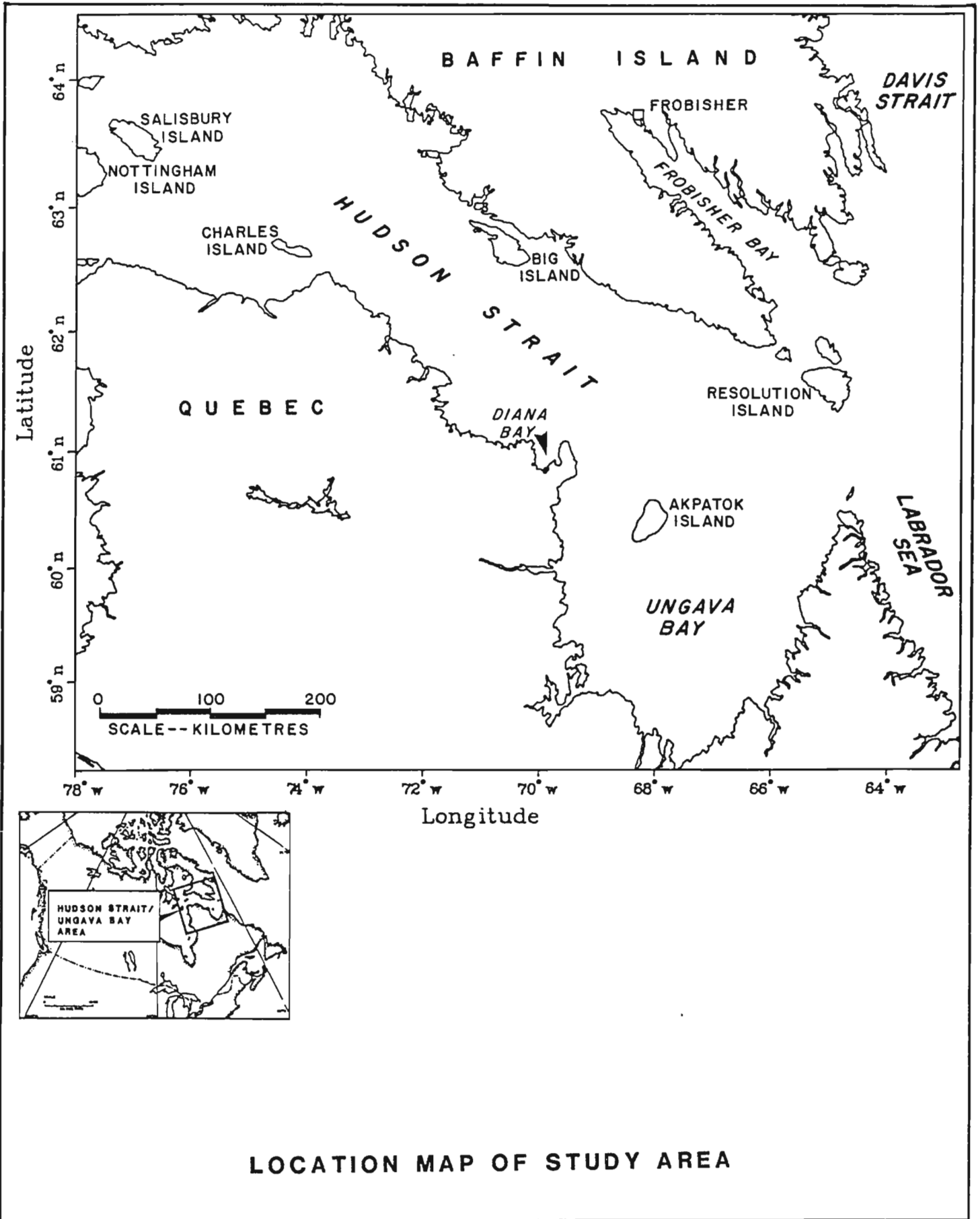


FIGURE 1

Hudson Strait and in Ungava Bay. A twenty-four day simulation, therefore, combining these four constituents was undertaken and the resulting time series examined using standard tidal analysis techniques (Foreman, 1979). The model results are presented in terms of cophase and coamplitude charts describing the water surface elevation for each constituent. Current vector plots of the dominant  $M_2$  tide at hour intervals throughout a tidal cycle (referenced to highwater at Diana Bay) are included and can be considered as representative of the overall current flow in the Hudson Strait/Ungava Bay study area.

## 2. BACKGROUND TIDAL INFORMATION

Descriptive information of the tides in Hudson Strait and Ungava Bay has been documented since the voyages of navigators such as John Davis in 1587. The area has gained a reputation for very strong tidal currents (in the order of 5 knots) and large tidal ranges (up to 15 m) (Canadian Hydrographic Service, 1983). The utilization of automatic data collection instruments has quantified the magnitude and direction of the currents and the variations in water elevation at several locations in this region. The Marine Environmental Data Service (MEDS) and the Canadian Hydrographic Service (CHS) has archived tidal elevation data gathered in the study area in the form of amplitude and phase for various tidal components including the four constituents of interest; the  $M_2$ ,  $S_2$ ,  $N_2$  and  $K_1$ . Figure 2 and Table 1 provide the location and the constituent values, respectively, for each of the tidal information stations in the Hudson Strait/Ungava Bay region. It should be noted that several of the data collection points (see Table 1) are represented by water elevation records of less than the 28 day period which is required to resolve the  $N_2$  component. At these locations the  $N_2$  constituent characteristics were determined by inference from the  $M_2$  data. The tides in the study area are mainly semi-diurnal with a typical amplitude ratio for the  $M_2:S_2:N_2:K_1$  of 100:33:20:5.

A cotidal chart describes the fields of amplitudes and phase lags for the water elevation of a given tidal constituent. Figure 3 shows two cotidal charts based on observations of the  $M_2$  tide at coastal stations in the study area (Dohler, 1966 and Godin, 1980). In each the solid contours represent cophase lines along which the vertical displacement of the  $M_2$  tide is simultaneous. The phases are measured in degrees and correspond to the phase lag at Eastern Standard Time (the time zone 5 hours ahead of Greenwich Mean Time, GMT + 5 hours). The tidal wave progresses in the direction of increasing phase and it can be seen that the tidal signal enters the Hudson Strait/Ungava Bay system at the

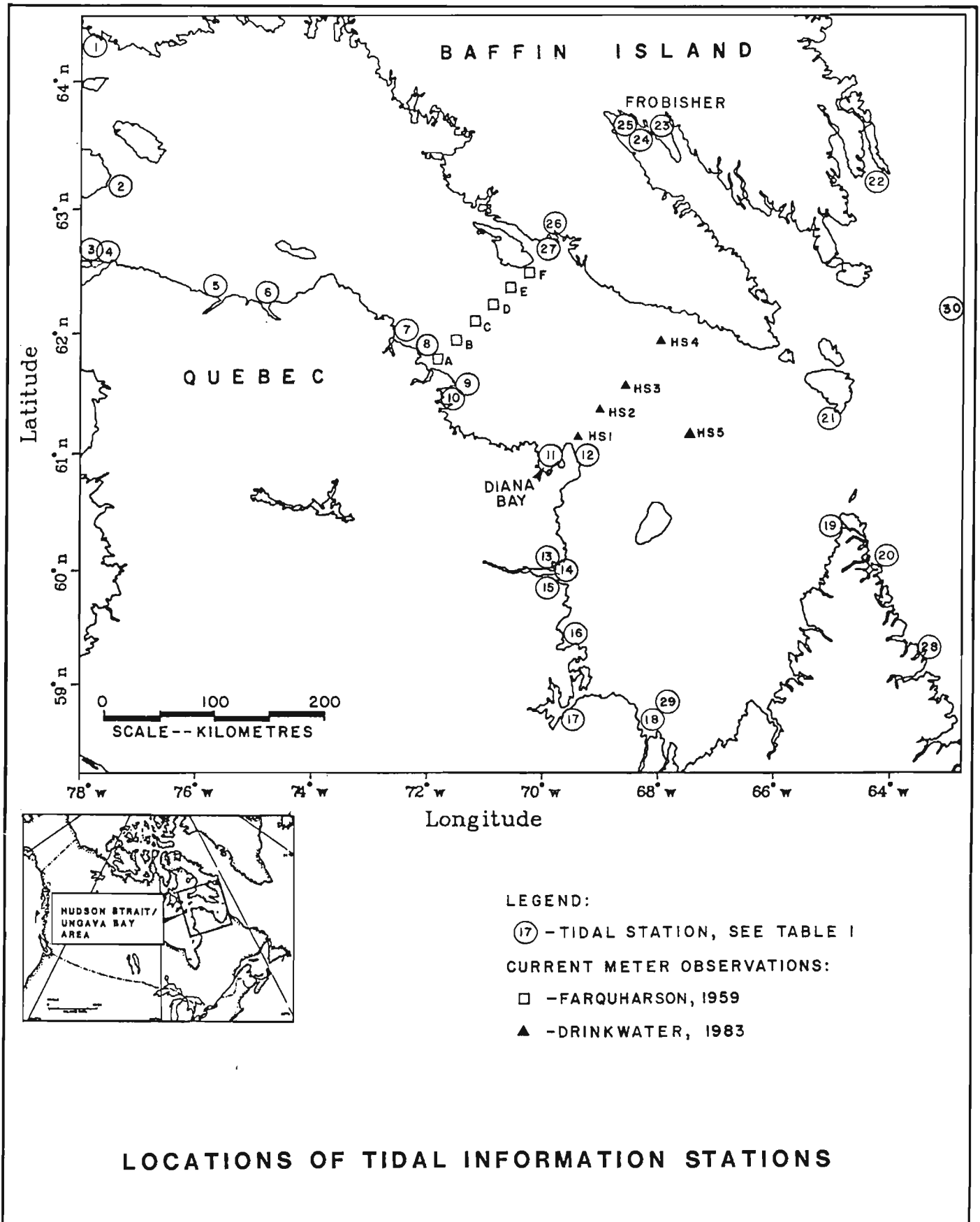


FIGURE 2

TABLE 1. TIDAL INFORMATION AT STATIONS WITHIN THE MODEL BOUNDARY  
DETERMINED FROM OBSERVED TIDAL DATA

	<u>Tidal Station</u>	<u>Constituent</u>	<u>Amplitude (cm)</u>	<u>Phase (degree) GMT +5 hrs</u>
1.	Schooner Harbour 62.4°N, 77.9°W	M <sub>2</sub>	207.5	316.0
		N <sub>2</sub>	41.4	289.6
		S <sub>2</sub>	71.0	9.0
		K <sub>1</sub>	8.2	147.0
2.	Port de Boucherville 63.2°N, 77.6°W	M <sub>2</sub>	144.4	270.0
		N <sub>2</sub>	27.4	331.6
		S <sub>2</sub>	53.9	326.0
		K <sub>1</sub>	6.7	113.0
3.	Port de LaPerriere * 62.6°N, 78.1°W	M <sub>2</sub>	94.1	268.0
		N <sub>2</sub>	18.2	332.6
		S <sub>2</sub>	37.7	322.0
		K <sub>1</sub>	4.2	66.0
4.	Digges Harbour 62.6°N, 77.9°W	M <sub>2</sub>	100.2	279.0
		N <sub>2</sub>	19.5	251.6
		S <sub>2</sub>	39.3	325.0
		K <sub>1</sub>	5.4	104.0
5.	Sugluk 62.2°N, 75.7°W	M <sub>2</sub>	155.1	255.0
		N <sub>2</sub>	30.7	227.6
		S <sub>2</sub>	58.5	304.0
		K <sub>1</sub>	10.0	90.0
6.	Deception Bay * 62.2°N, 74.8°W	M <sub>2</sub>	171.7	248.2
		N <sub>2</sub>	34.3	222.6
		S <sub>2</sub>	60.3	304.0
		K <sub>1</sub>	8.3	83.0
7.	Douglas Harbour 61.9°N, 72.6°W	M <sub>2</sub>	259.3	231.0
		N <sub>2</sub>	48.1	214.6
		S <sub>2</sub>	92.0	298.0
		K <sub>1</sub>	10.5	60.0
8.	Wakeham Bay 61.6°N, 72.3°W	M <sub>2</sub>	336.5	234.0
		N <sub>2</sub>	69.6	212.0
		S <sub>2</sub>	162.6	279.1
		K <sub>1</sub>	13.4	77.2
9.	Doctor Island * 61.7°N, 71.6°W	M <sub>2</sub>	257.5	237.0
		N <sub>2</sub>	51.5	310.6
		S <sub>2</sub>	87.4	289.0
		K <sub>1</sub>	14.9	118.0



TABLE 1. continued

	<u>Tidal Station</u>	<u>Constituent</u>	<u>Amplitude (cm)</u>	<u>Phase (degree) GMT + 5 hrs</u>
10.	Stupart Bay * 61.6°N, 71.5°W	M <sub>2</sub>	274.9	225.0
		N <sub>2</sub>	54.8	331.6
		S <sub>2</sub>	92.9	282.0
		K <sub>1</sub>	14.3	99.0
11.	Diana Bay 60.9°N, 70.1°W	M <sub>2</sub>	293.0	224.2
		N <sub>2</sub>	58.6	198.0
		S <sub>2</sub>	99.3	275.5
		K <sub>1</sub>	15.7	87.9
12.	Koartac 61.1°N, 69.6°W	M <sub>2</sub>	266.5	253.9
		N <sub>2</sub>	51.1	226.2
		S <sub>2</sub>	91.8	311.3
		K <sub>1</sub>	6.8	122.1
13.	Basking Island 60.0°N, 70.1°W	M <sub>2</sub>	316.6	253.0
		N <sub>2</sub>	58.8	235.0
		S <sub>2</sub>	99.9	313.0
		K <sub>1</sub>	14.3	112.0
14.	Pikiyulik Island 60.0°N, 69.9°W	M <sub>2</sub>	304.8	251.0
		N <sub>2</sub>	55.1	224.0
		S <sub>2</sub>	94.7	302.0
		K <sub>1</sub>	14.9	105.0
15.	Agvik Island 60.0°N, 69.7°W	M <sub>2</sub>	349.3	225.0
		N <sub>2</sub>	64.6	199.0
		S <sub>2</sub>	117.0	275.0
		K <sub>1</sub>	17.6	110.0
16.	Hopes Advance Bay 59.4°N, 69.6°W	M <sub>2</sub>	388.3	225.0
		N <sub>2</sub>	83.2	188.0
		S <sub>2</sub>	125.2	280.0
		K <sub>1</sub>	20.7	97.0
17.	Leaf Basin 58.7°N, 69.8°W	M <sub>2</sub>	433.1	251.0
		N <sub>2</sub>	91.7	253.0
		S <sub>2</sub>	136.5	314.0
		K <sub>1</sub>	18.5	113.0
18.	Koksoak River Entrance 58.7°N, 68.2°W	M <sub>2</sub>	408.7	229.0
		N <sub>2</sub>	75.8	196.0
		S <sub>2</sub>	135.9	282.0
		K <sub>1</sub>	15.8	91.0

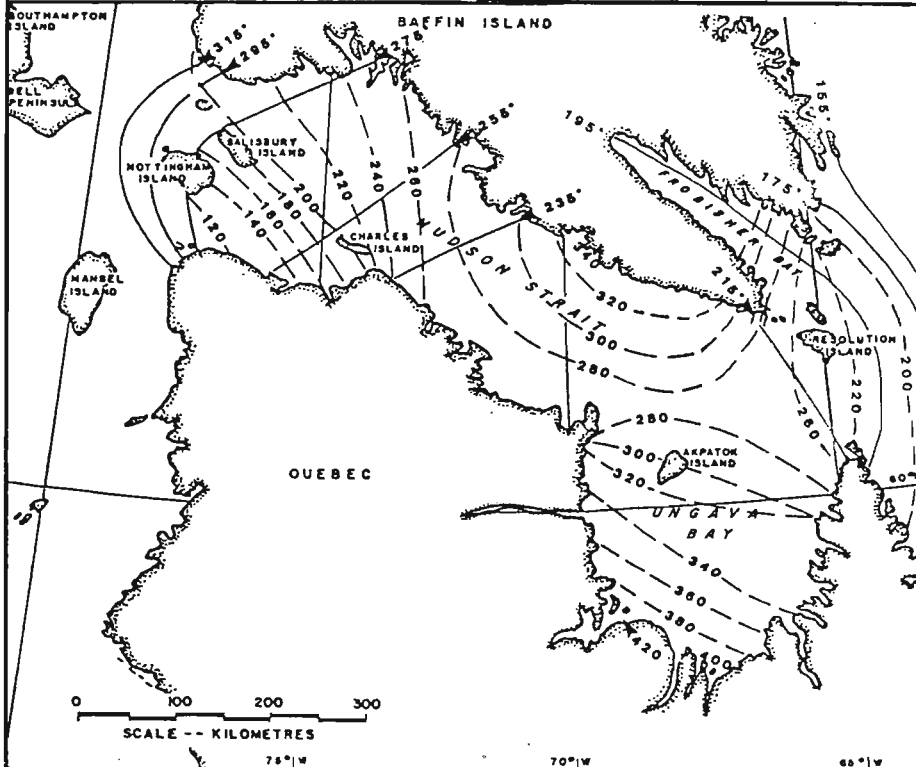
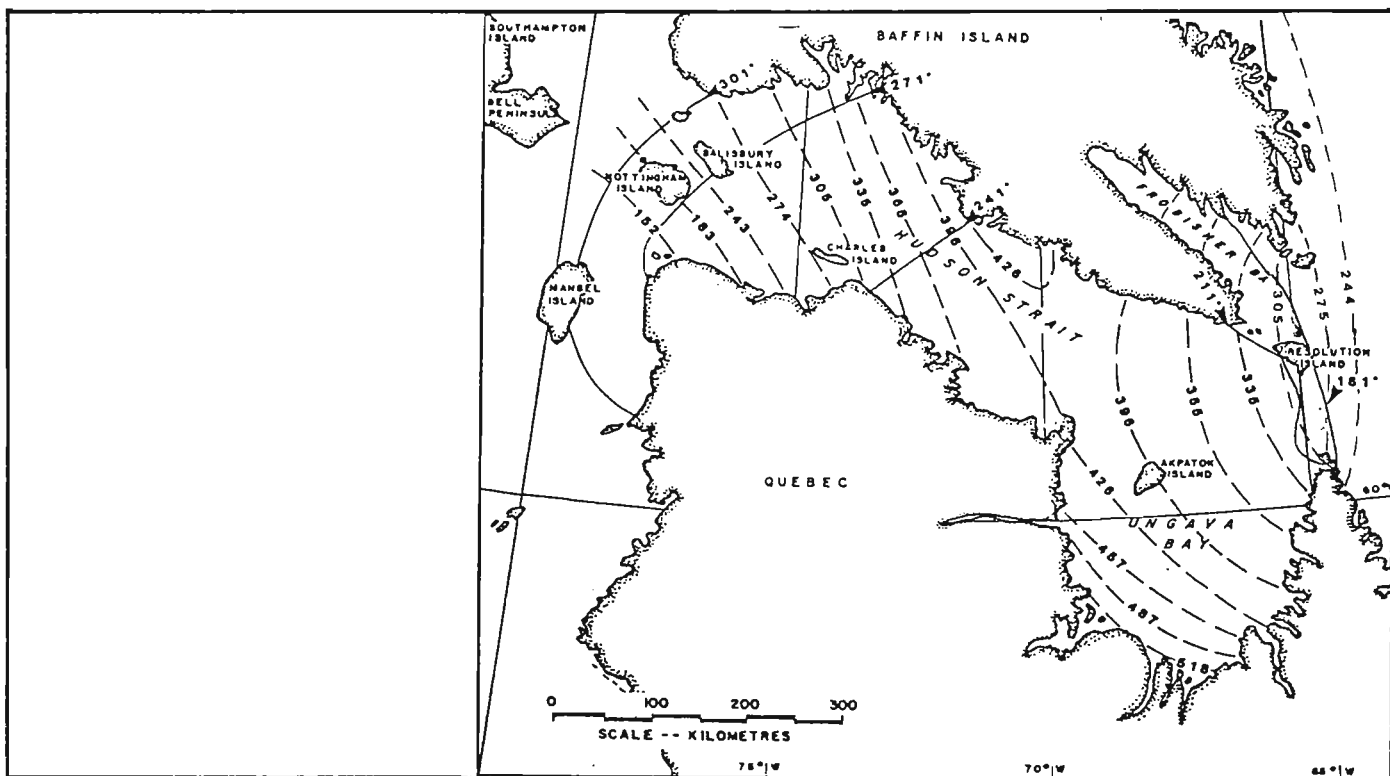
TABLE 1. continued

	<u>Tidal Station</u>	<u>Constituent</u>	<u>Amplitude (cm)</u>	<u>Phase (degree) GMT +5 hrs</u>
19.	Port Burwell 60.4°N, 64.9°W	M <sub>2</sub>	214.2	209.0
		N <sub>2</sub>	42.0	177.6
		S <sub>2</sub>	65.2	258.0
		K <sub>1</sub>	12.4	90.0
20.	Williams Harbour *	M <sub>2</sub>	98.1	187.5
		N <sub>2</sub>	30.1	154.4
		S <sub>2</sub>	23.7	227.0
		K <sub>1</sub>	19.2	72.5
21.	Acadia Cove * (Easton, 1972) 61.6°N, 64.73°W	M <sub>2</sub>	216.0	211.0
		N <sub>2</sub>	43.0	-
		S <sub>2</sub>	89.0	246.0
		K <sub>1</sub>	13.0	115.0
22.	Brevoort Harbour 63.3°N, 64.2°W	M <sub>2</sub>	180.7	157.0
		N <sub>2</sub>	34.7	132.6
		S <sub>2</sub>	64.0	195.0
		K <sub>1</sub>	17.0	49.0
23.	Frobisher S Farthest 63.5°N, 68.0°W	M <sub>2</sub>	329.5	218.5
		N <sub>2</sub>	54.0	188.6
		S <sub>2</sub>	110.4	267.1
		K <sub>1</sub>	18.0	100.6
24.	Resor Island 63.2°N, 68.1°W	M <sub>2</sub>	334.3	197.0
		N <sub>2</sub>	66.4	168.6
		S <sub>2</sub>	118.8	242.0
		K <sub>1</sub>	20.1	96.0
25.	Frobisher 63.7°N, 68.5°W	M <sub>2</sub>	345.2	193.1
		N <sub>2</sub>	67.7	164.7
		S <sub>2</sub>	117.4	238.8
		K <sub>1</sub>	18.4	85.5
26.	Lake Harbour 62.9°N, 69.9°W	M <sub>2</sub>	349.6	231.7
		N <sub>2</sub>	67.6	204.4
		S <sub>2</sub>	119.9	280.9
		K <sub>1</sub>	15.2	102.1
27.	Ashe Inlet 62.6°N, 70.6°W	M <sub>2</sub>	335.2	230.0
		N <sub>2</sub>	67.0	208.6
		S <sub>2</sub>	121.3	287.0
		K <sub>1</sub>	15.8	103.0

TABLE 1. continued

	<u>Tidal Station</u>	<u>Constituent</u>	<u>Amplitude (cm)</u>	<u>Phase (degree) GMT +5 hrs</u>
28.	Schooner Cove * 59.1°N, 63.5°W	M <sub>2</sub>	35.2	180.1
		N <sub>2</sub>	9.1	188.4
		S <sub>2</sub>	13.7	207.8
		K <sub>1</sub>	14.2	95.5
29.	Ungava Bay 58.6°N, 68.2°W	M <sub>2</sub>	420.7	232.9
		N <sub>2</sub>	-	205.7
		S <sub>2</sub>	133.3	283.9
		K <sub>1</sub>	17.7	91.8
30.	Hekja Wellsite 62.2°N, 62.9°W	M <sub>2</sub>	160.0	171.0
		N <sub>2</sub>	35.0	151.0
		S <sub>2</sub>	53.0	207.0
		K <sub>1</sub>	12.0	83.0

\* Recorded tidal data less than 28 days; inference of N<sub>2</sub> parameters from M<sub>2</sub> data undertaken.



SOURCE: DOHLER, 1966

SOURCE: GODIN, 1960

**LEGEND:**

--- COAMPLITUDE (Cm)

— COPHASE (DEGREES)

TIME ZONE: GMT+5HRS.

**COTIDAL CHARTS FOR THE M2 TIDE  
IN HUDSON STRAIT/UNGAVA BAY**

FIGURE 3

eastern entrance and propagates westward through the Strait. The dashed lines denote contours of equal amplitude with units of centimetres. Extreme amplitudes in the semidiurnal tide in Ungava Bay result from the effects of resonance in the system and a near absence of cophase lines indicating simultaneous tides over a large area. It is evident that there are discrepancies, particularly in the amplitude, between the two representations of the tidal regime shown in Figure 3. The results of the numerically generated cotidal charts will be used to resolve the differences between these two interpretations of the observed coastal tidal information.

To complete the description of the tidal movement in the study area the cotidal charts, which represent the vertical tide only, must be supplemented by information of the horizontal tidal current. In the study area two field investigations (Farquharson, 1959 and Drinkwater, 1983) have provided current observations of sufficient duration, and taken at enough depths, to resolve the tidal variations in flow and their vertical structure. The results of these observations are detailed in Section 4 and compared to the current values calculated by the numerical model. The field studies show that the currents are nearly uniform with depth implying that the depth averaged results generated numerically should be appropriate for the region. Drinkwater's analysis also shows that tides are a dominating source of currents in Hudson Strait making the results of tidal circulation modelling of particular interest.

### 3. THE BAROTROPIC TIDAL MODEL

A two-dimensional numerical model (Martec/AOL model) used to assess tidally driven barotropic flow was applied to the Hudson Strait/Ungava Bay study area. The model structure is comprised of depth averaged equations of continuity and motion discretized in a semi-implicit manner on a Richardson lattice (Martec, 1983). Spherical coordinates are used to accommodate areas of large latitudinal extent and are appropriate for the study area centered at 62°N latitude.

The new application of the model to the Hudson Strait/Ungava Bay area entails the digitization of the bathymetry of the region. To solve for the tidal circulation also requires the specifications of tidal elevations along open ocean boundaries and the adjustment of friction factors which simulate natural energy dissipation. The maximum depth in the model is 1,000 m, the minimum grid spacing X (east-west) and Y (north-south) are 12.5 and 11.1 km, respectively, yielding a maximum time step of 84 seconds, in order to preserve numerical stability of the semi-implicit integration scheme. The actual time step used in the model runs was 62.1 seconds, one lunar minute for the M<sub>2</sub> simulations and 60 seconds for the combined M<sub>2</sub>, N<sub>2</sub>, S<sub>2</sub>, K<sub>1</sub> runs.

The model grid is comprised of elements 6 minutes in latitude by 15 minutes in longitude giving a total of 3,843 grid points for the study area. Figure 4 illustrates the model domain superimposed on the study area coastline. Grid elements on the model periphery are defined as either a land or an open ocean point and dictate the flow characteristics at the model boundaries.

#### 3.1 Digitization of the Model Bathymetry

Bathymetric information for the model was derived from soundings provided by the Canadian Hydrographic Service (Hudson Strait Chart No. 5450, Davis Strait Chart No. 7011, and Ungava Bay Chart No. 5300). All

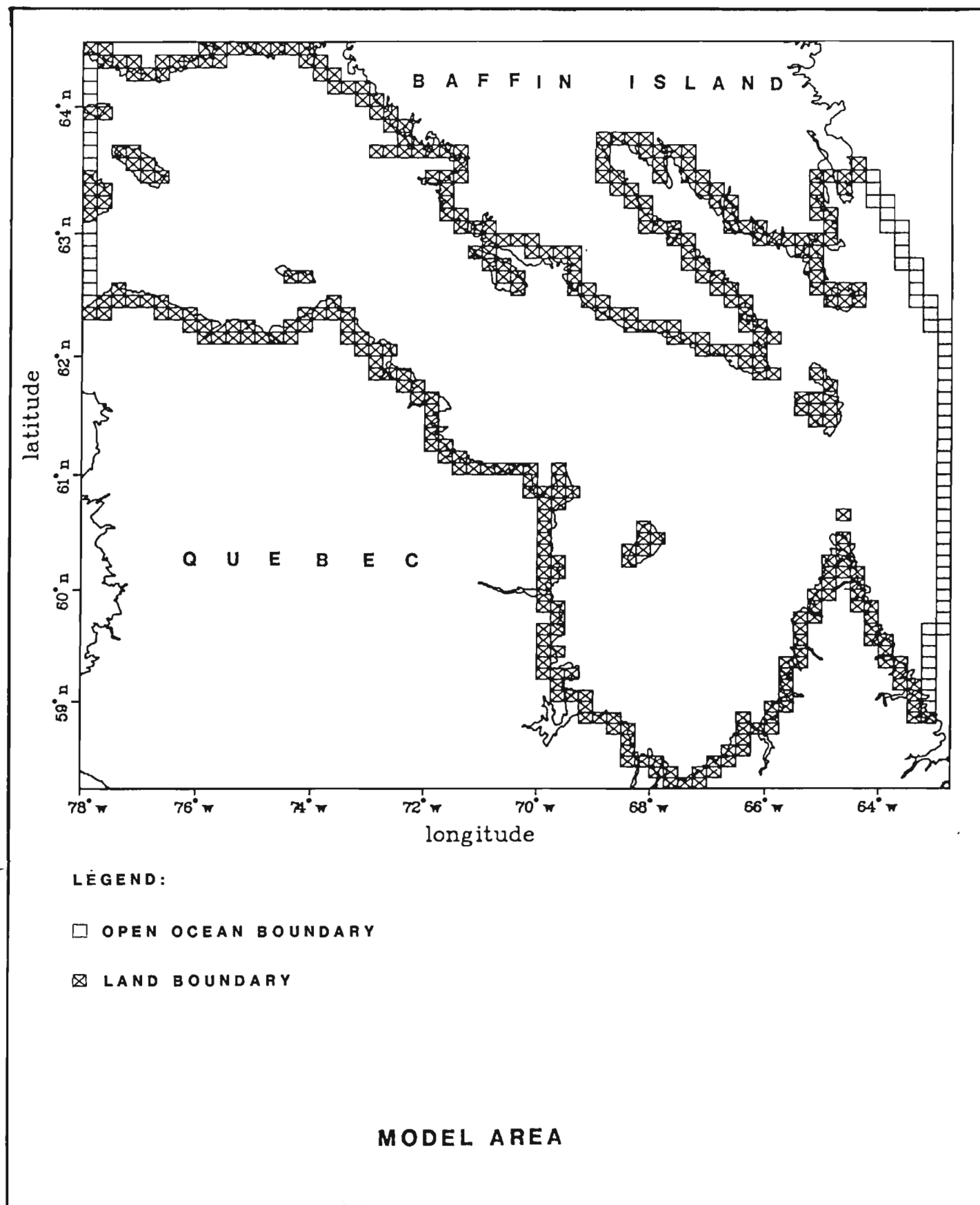


FIGURE 4

depth soundings recorded on the chart and within the model area were digitized and archived in computer files as three numbers representing latitude, longitude, and depth. This data file was then manipulated to obtain a representative depth for each grid element. If several soundings were given within a specific grid element, the arithmetic mean of these soundings was used as the representative depth. If no bathymetric data were available for a specific grid element, a value was estimated from the adjacent depth data and the general character of the surrounding topography.

Grid elements with no available measured soundings were recognized as potential sources of error in the model results. Therefore, the model sensitivity to depth changes in the regions of estimated bathymetry was examined by modifying the depth and observing the resulting effect on the simulated  $M_2$  tide. This aspect of the study is discussed in detail in Section 4.

Figure 5 is a model generated bathymetric map of the study area and shows isobath contours of 100 m and 350 m. Also indicated are the grid elements at which depth data were not available and thus required manual specification.

### 3.2 Model Boundary Conditions and Calibration

To solve the numerical problem for tidally driven flows one must specify tidal elevations along open ocean boundaries and also select values for the free parameters appearing in the equations of motion programmed in the model. The intent of the calibration is to adjust these factors to optimize the agreement between modelling results and tidal observations. Ideally observed tidal data on the open ocean boundaries would be available and specified as input into the model, without the need for further adjustments. However, in the case of the Hudson Strait/Ungava Bay model, tidal stations are sparse, especially near the eastern boundary, and in addition some of the available data is of



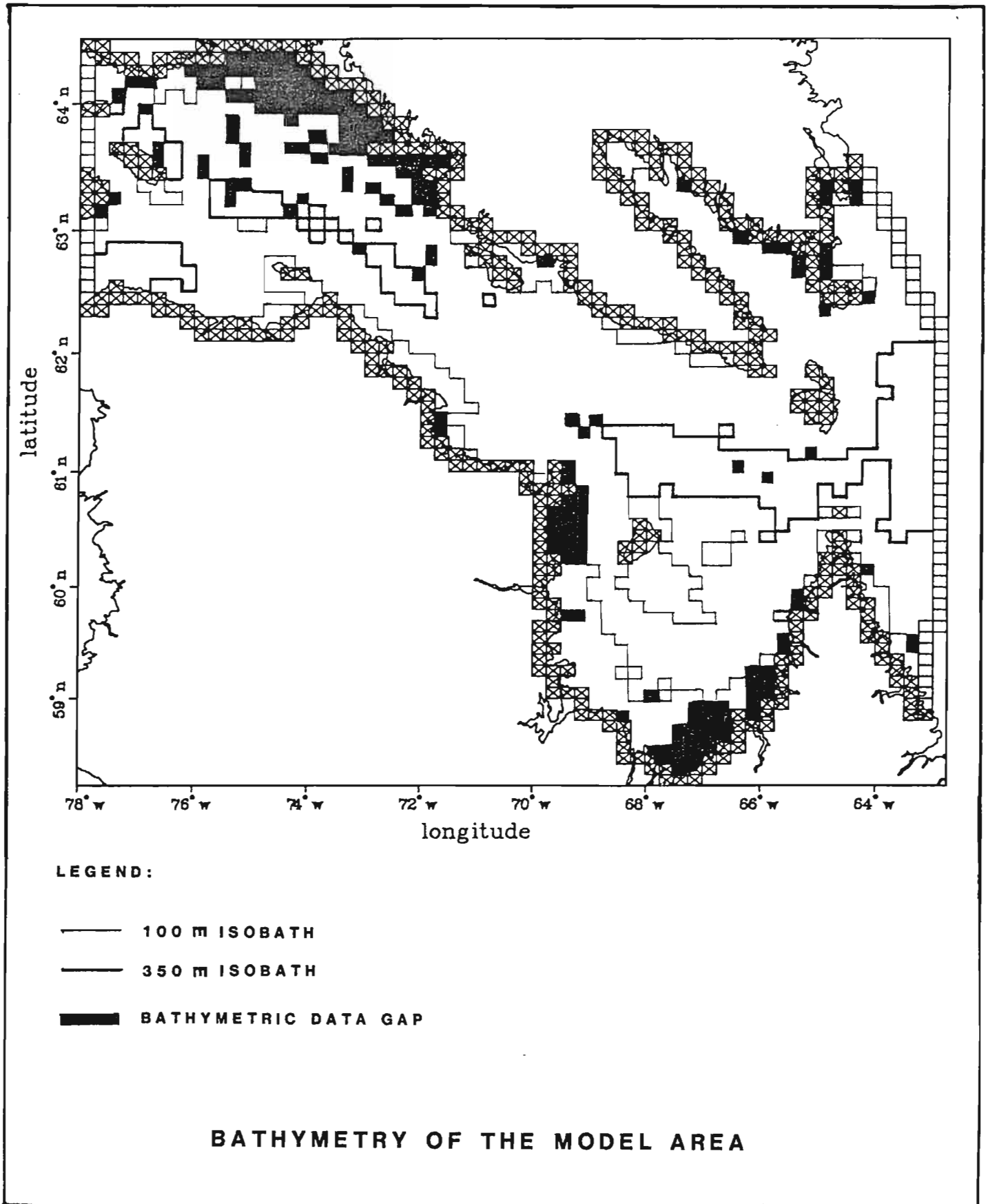


FIGURE 5

questionable accuracy. Therefore use has been made of existing cotidal charts (Godin, 1980) to complement available data and provide a consistent match between the numerically generated flow field and the tidal behavior outside of the modelled region.

A region of noticeable uncertainty in the observed tidal data is the Resolution Island area where the tide tables suggest very rapid changes in phase (one hour difference between the two sides of the island, roughly 40 km). Several initial model runs with boundaries close to this area have shown that a change of phase of  $30^\circ$  at Resolution can cause amplitude changes up to 10% as well as phase changes of  $20^\circ$  at the model interior. Consequently, the final boundaries were selected further east into the Davis Strait/Labrador Sea in order to freely calculate the evidently dynamic tidal regime at the eastern entrance to Hudson Strait without constraints and potential 'numerical noise' imposed by nearby boundaries. The results of model runs using an eastern boundary along the  $60^\circ\text{W}$  meridian indicated that the accurate specification of tidal elevation along the open boundary was greatly complicated by the lack of offshore tidal data and the presence of a degenerate amphidromic point along the Labrador coast near  $59^\circ\text{N}$ . The final eastern boundary was therefore established along the  $63^\circ\text{W}$  meridian where available information at Brevoort Harbour, the Hekja wellsite and Schooner Cove could be utilized to advantage. The boundary conditions adopted for the final model runs are given in Table 2.

As described in the documentation of the barotropic model (Martec, 1984b) there are generally three free parameters, namely  $A_h$ ,  $V$  and  $K$  to be specified for a model run.  $A_h$ , the coefficient of horizontal eddy viscosity, is parameterized in terms of the water depth (following Schwiderski, 1980). The specification of eddy viscosity is necessary to preserve numerical stability in the model but it can be readily shown to have negligible effect on the tidal circulation on the scale of the model resolution.  $V$  represents the magnitude of currents not attributable to the tidal constituents under analysis and may be

TABLE 2. MODEL BOUNDARY CONDITIONS

	<u>Location</u>	<u>Constituent</u>	<u>Amplitude (cm)</u>	<u>Phase (degree) GMT +5 hrs</u>
1.	63.5°N, 64.1°W Breevort Harbour	M <sub>2</sub>	181	157
		N <sub>2</sub>	35	133
		S <sub>2</sub>	64	195
		K <sub>1</sub>	17	49
2.	62.2°N, 62.9°W Davis Strait (Hekja wellsite)	M <sub>2</sub>	160	171
		N <sub>2</sub>	35	151
		S <sub>2</sub>	53	207
		K <sub>1</sub>	12	83
3.	60.3°N, 62.9°W Labrador Sea	M <sub>2</sub>	100	184
		N <sub>2</sub>	22	171
		S <sub>2</sub>	33	208
		K <sub>1</sub>	13	90
4.	59.1°N, 63.5°W Schooner Cove	M <sub>2</sub>	35	180
		N <sub>2</sub>	9	188
		S <sub>2</sub>	14	208
		K <sub>1</sub>	14	96
5.	62.6°N, 77.9°W Southern Digges Island	M <sub>2</sub>	100	280
		N <sub>2</sub>	20	252
		S <sub>2</sub>	39	325
		K <sub>1</sub>	5	104
6.	63.0°, 77.9°W Southern Nottingham Island	M <sub>2</sub>	144	270
		N <sub>2</sub>	27	258
		S <sub>2</sub>	54	326
		K <sub>1</sub>	7	120
7.	64.4°N, 77.9°N Schooner Harbour	M <sub>2</sub>	208	316
		N <sub>2</sub>	41	290
		S <sub>2</sub>	71	9
		K <sub>1</sub>	8	147

estimated from observations. This parameter becomes significant only when modelling the minor tidal components individually to account for the influence of the dominant  $M_2$  tide. The only free parameter remaining is the bottom friction factor  $K$  which is iteratively adjusted to optimize the agreement between observed tidal data and the model results. It can be noted that any error in the estimated  $V$  can be compensated for by the choice of  $K$ , since both occur together in the equations of motion. The optimal values of the friction parameters used for the final model runs are discussed in the following section.

### 3.3 Model Implementation for the Hudson Strait/Ungava Bay Study Area

The Martec/AOL barotropic tidal model was adapted to run on the CRAY computer of Dorval, P.Q. for the present study. The final plotting of the model results was accomplished using the DISSPLA package on the Cyber computer at the Bedford Institute of Oceanography.

The original structure of the numerical model was refined in several aspects to more accurately simulate the physical conditions in the Hudson Strait/Ungava Bay study area. The first of these was the inclusion of a tidal generating force (TGF) into the equations governing the water motion. With this addition the tidal forcing of the model is provided by two sources: by the tidal signal entering at the open ocean boundaries, and also by the TGF within the Hudson Strait/Ungava Bay waters. However, inclusion of the TGF into the model showed less than a one percent change in the  $M_2$  tidal amplitude and consequently was considered too small to be included in the simulations of the other tidal constituents. A dimensional analysis of the equations of motion confirmed that the TGF effects should be minimal.

A second enhancement in the numerical model was the capability of dealing with drying model elements. In the event that the model predicts that the water level should fall below the depth of a grid element, no further flow is allowed to leave the element until the

following tide causes a new rise in water level. In this way the model remains stable and does not predict physically meaningless negative water depth.

In order to analyze the results of simulations of several constituents modelled simultaneously a tidal analysis post processor was developed. Harmonic analysis techniques, used in earlier stages of the study to determine tidal phases and amplitudes, were not applicable to situations where the time series to be analyzed contained several distinct frequencies. The present model uses a least squares fitting technique derived from Foreman (1979) for tidal analysis. Nodal modulation corrections usually included for the analysis of tidal records is not included since the model results do not include long term modulations of semi-diurnal and diurnal constituents. Initially simulation of the  $M_2$ ,  $N_2$ ,  $S_2$  and  $K_1$  tidal regime were undertaken independently. The agreement between predicted and observed tides was optimized by fine tuning the values for the quadratic bottom friction factor and the background flow velocity used to simulate linear friction effects. For the principal tidal constituent the model results were relatively sensitive to the friction factor, with phase lags in Ungava Bay typically increasing by  $15^\circ$  or half an hour for a .0005 increase in drag coefficient. The best fit value for the  $M_2$  tide given below agrees with that used by Easton (1972) and Griffiths *et al.* (1981) in their numerical studies of the same regions. For the minor semidiurnal constituents, the friction factor had to be significantly increased, which is expected due to interaction with the strong  $M_2$  tide. The fit for the  $S_2$  and  $N_2$  were slightly better with strong bottom friction factor and low background velocity; however, the model showed very little sensitivity to using quadratic or linear friction, as long as a change in one was compensated by a change in the other. For the  $K_1$  tide the best agreement was found with the same drag coefficient as the  $M_2$  tide but with a background velocity of 50 cm/sec. The optimal values of the friction parameters used for the final model runs are given below.

<u>Constituent</u>	<u>Bottom Friction Factor</u>	<u>Background Velocity for Bottom Friction (cm/sec)</u>
M <sub>2</sub>	0.0025	0
S <sub>2</sub>	0.0100	0
N <sub>2</sub>	0.0150	0
K <sub>1</sub>	0.0025	50

The results of these independent tidal constituent simulations are available under separate cover (Martec, 1984a).

### 3.4 Simulation of the Combined M<sub>2</sub>, N<sub>2</sub>, S<sub>2</sub> and K<sub>1</sub> Tidal Regime

The barotropic model has the capacity to simulate the propagation of the tide at more than one frequency simultaneously. Modelling the four tidal constituents (M<sub>2</sub>, S<sub>2</sub>, N<sub>2</sub> and K<sub>1</sub>) at one time, instead of individually as done previously, allows for the non-linear interaction between the constituents. The simulation period for this combined constituent run covered twenty-four days providing a time series of water elevation for each grid element in the model. A tidal analysis (following Foreman, 1979) was conducted at each point to resolve the individual contributions of the M<sub>2</sub>, S<sub>2</sub>, N<sub>2</sub> and K<sub>1</sub> constituents. The results of the tidal analysis are presented in the form of charts of cotidal lines and tidal ellipses for each of the four constituents in the Hudson Strait/Ungava Bay system. Appendix I includes a tabulation of observed and modelled values of phase and amplitude.

## 4. MODEL RESULTS

### 4.1 Tidal Elevations

The comparison between the modelled tidal amplitude and phase and observations was carried out for several key locations in the Hudson Strait/Ungava Bay system. The choice of which stations to use as reference points was based on:

1. The duration and reliability of observations at the station; and
2. A geographical location free from local features not resolved by the model.

For instance, the tidal record from Basking Island is dismissed because its position in an estuary is too small to be resolved by the model. Tables 3 and 4 list the final reference stations, the tidal characteristics produced by the model, and the differences between the observed and modelled values. A comparison between all available observations and the model result for the nearest grid points is given in Appendix I. The stations in Appendix I were not used in the calibration of the model as reference points and therefore constitute an independent check on model results. The numerical results of both the independent and combined constituent runs were examined for each tidal component. It was expected that the results of the combined frequencies would compare more favourably to the observed data than would the independent runs for all of the constituents. However, it was found that an independent simulation for the  $M_2$  tide gave better agreement with observed  $M_2$  amplitudes than did the results of a combined  $M_2/N_2/S_2/K_1$  simulation. The combined forcing was, however, superior in simulating the tidal regimes of the other constituents. Final results for the  $M_2$  tide are therefore derived from independent  $M_2$  runs, and results for the  $N_2$ ,  $S_2$ , and  $K_1$  simulations are from the combined  $M_2/N_2/S_2/K_1$  constituent runs. Figures 6 to 9 are cotidal charts of water elevation for each of the

TABLE 3. COMPARISON OF AMPLITUDES OF OBSERVED AND MODELLED TIDES (cm)

Location	Observed/Modelled Amplitude	Real Difference	Percentage Difference	Observed/Modelled Amplitude	Real Difference	Percentage Difference
	M <sub>2</sub>			S <sub>2</sub>		
Ashe Inlet	335.2/327.0	-8.2	-2.4	121.3/99.8	-21.5	-17.7
Acadia Cove	216.0/219.2	3.2	1.5	89.0/73.7	-15.3	-17.2
Koksoak River Entrance	408.7/417.7	9.0	2.2	135.9/113.7	-22.2	-16.3
Hopes Advance Bay	388.3/388.2	-0.1	0.0	125.2/110.8	-14.4	-11.5
Diana Bay	293.0/293.1	0.1	0.9	99.3/82.1	-17.2	-17.3
Stupart Bay	274.9/275.0	0.1	0.0	92.9/82.3	-10.6	-11.4
Doctor Island	257.5/271.0	13.5	5.2	87.4/80.6	-6.8	-7.8
Sugluk	155.1/156.8	1.7	1.1	58.5/58.3	-0.2	-0.3
Port de Boucherville	144.4/143.9	-0.5	-0.3	53.9/54.0	0.1	0.2
Ungava Bay	420.7/423.4	2.7	0.6	133.3/113.3	-20.0	-15.0
	N <sub>2</sub>			K <sub>1</sub>		
Ashe Inlet	67.0/66.9	-0.1	-0.1	15.8/14.3	-1.5	-9.5
Acadia Cove	43.0/44.0	1.0	2.3	13.0/15.2	2.2	16.9
Koksoak River Entrance	75.8/75.9	0.1	0.1	15.8/16.0	0.2	1.3
Hopes Advance Bay	83.2/75.9	-7.3	-8.8	20.7/15.9	-4.8	-23.2
Diana Bay	58.6/58.5	-0.1	-0.2	15.7/14.0	-1.7	-10.8
Stupart Bay	54.8/54.9	0.1	0.	14.3/11.8	-2.5	-17.5
Doctor Island	51.5/54.3	2.8	5.4	14.9/12.0	-2.9	-19.5
Sugluk	30.7/30.7	0.0	0.0	10.0/7.0	-3.0	-30.0
Port de Boucherville	27.4/27.0	-0.4	-1.5	6.7/6.6	-0.1	-1.5
Ungava Bay	-/79.1	-	-	17.7/16.1	-1.6	-9.0



TABLE 4. COMPARISON OF PHASES OF OBSERVED AND MODELLED TIDES (degrees)

Location	Observed/Modelled	Real	Observed/Modelled	Real
	Phase	Difference	Phase	Difference
		M <sub>2</sub>		S <sub>2</sub>
Ashe Inlet	230.0/229.0	1.0	287.0/284.0	3.0
Acadia Cove	211.0/198.0	13.0	246.0/244.0	-2.0
Koksoak River Entrance	229.0/228.0	1.0	282.0/284.0	-2.0
Hopes Advance Bay	225.0/219.0	6.0	280.0/268.0	12.0
Diana Bay	224.2/218.0	6.2	275.5/269.0	6.5
Stupart Bay	225.0/224.0	1.0	282.0/280.0	2.0
Doctor Island	237.0/226.0	11.0	289.0/284.0	5.0
Sugluk	255.0/250.0	5.0	304.0/310.0	-6.0
Port de Boucherville	270.0/270.0	0.0	326.0/326.0	0.0
Ungava Bay	232.9/230.0	0.8	283.9/273.0	3.0
		N <sub>2</sub>		K <sub>1</sub>
Ashe Inlet	208.6/210.0	-1.4	103.0/100.0	3.0
Acadia Cove	- /174.0	-	115.0/87.0	28.0
Koksoak River Entrance	196.0/210.0	-14.0	91.0/92.0	91.0
Hopes Advance Bay	188.0/204.0	-16.0	97.0/89.0	8.0
Diana Bay	198.0/202.0	-4.0	87.9/86.0	1.9
Stupart Bay	331.6/209.0	122.6	99.0/87.0	12.0
Doctor Island	310.6/210.0	100.0	118.0/88.0	30.0
Sugluk	227.6/235.0	-7.4	90.0/94.0	-4.0
Port de Boucherville	331.6/258.0	73.6	113.0/118.0	-5.0
Ungava Bay	205.7/208.0	-0.6	91.8/92.0	-0.1

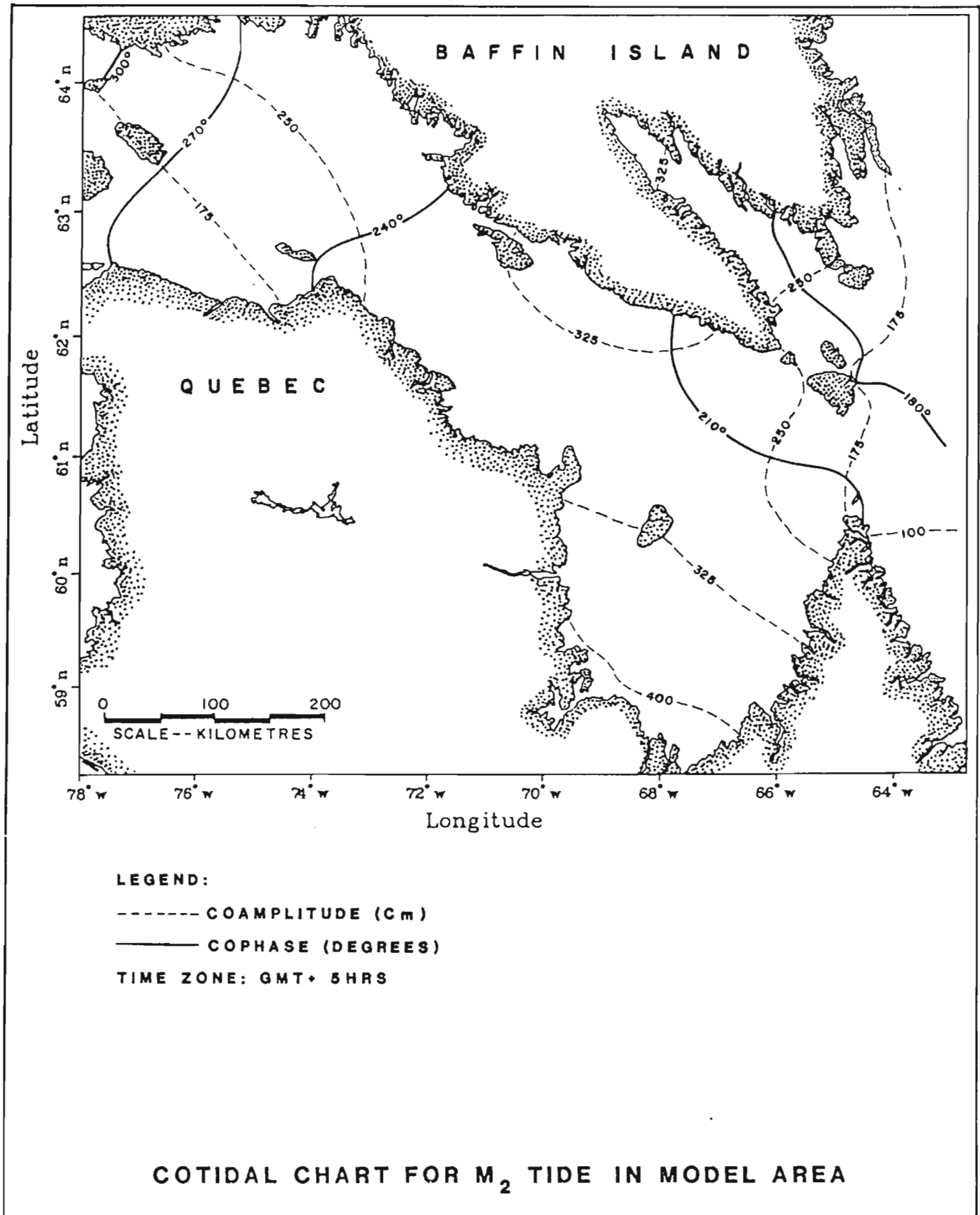


FIGURE 6

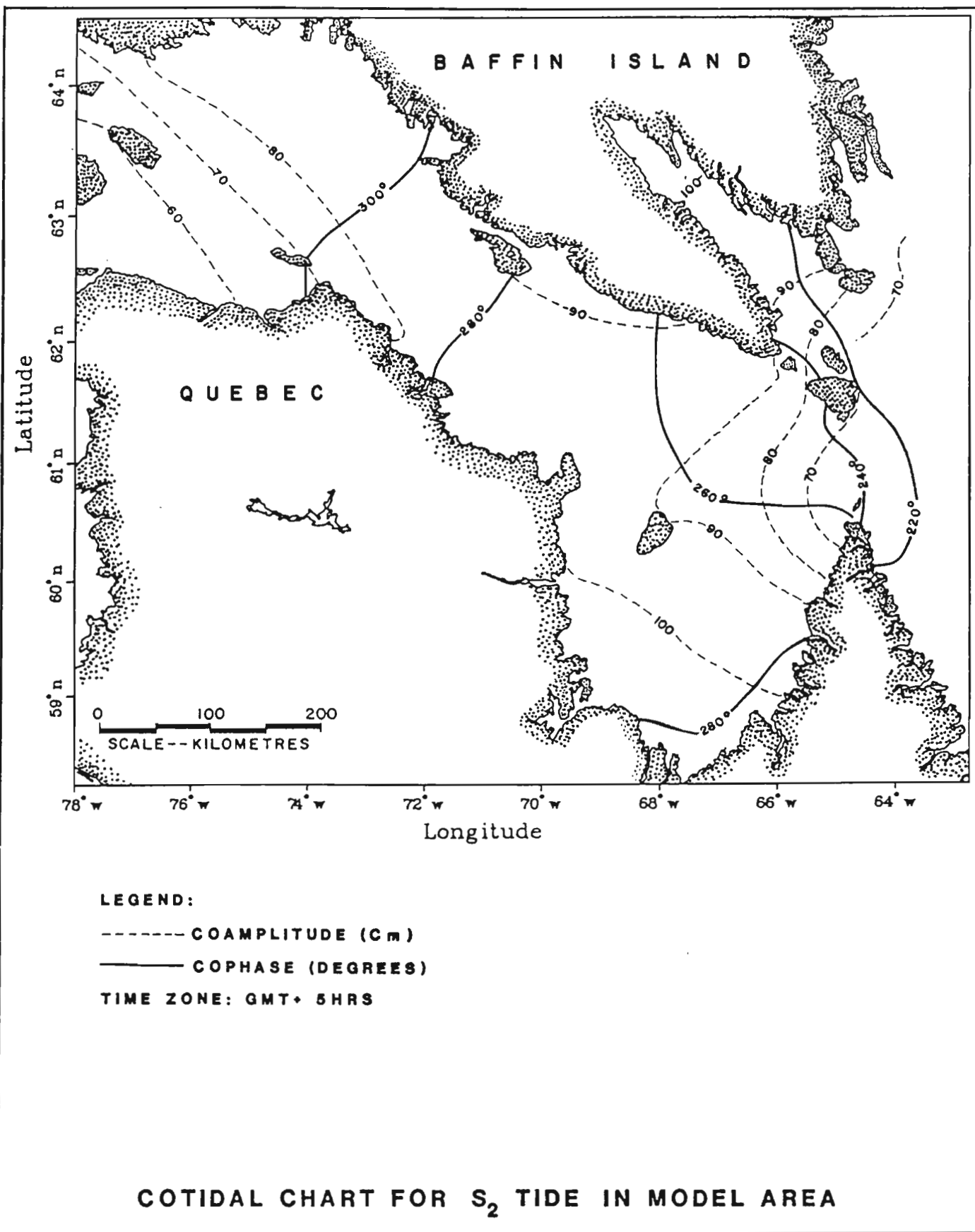


FIGURE 7

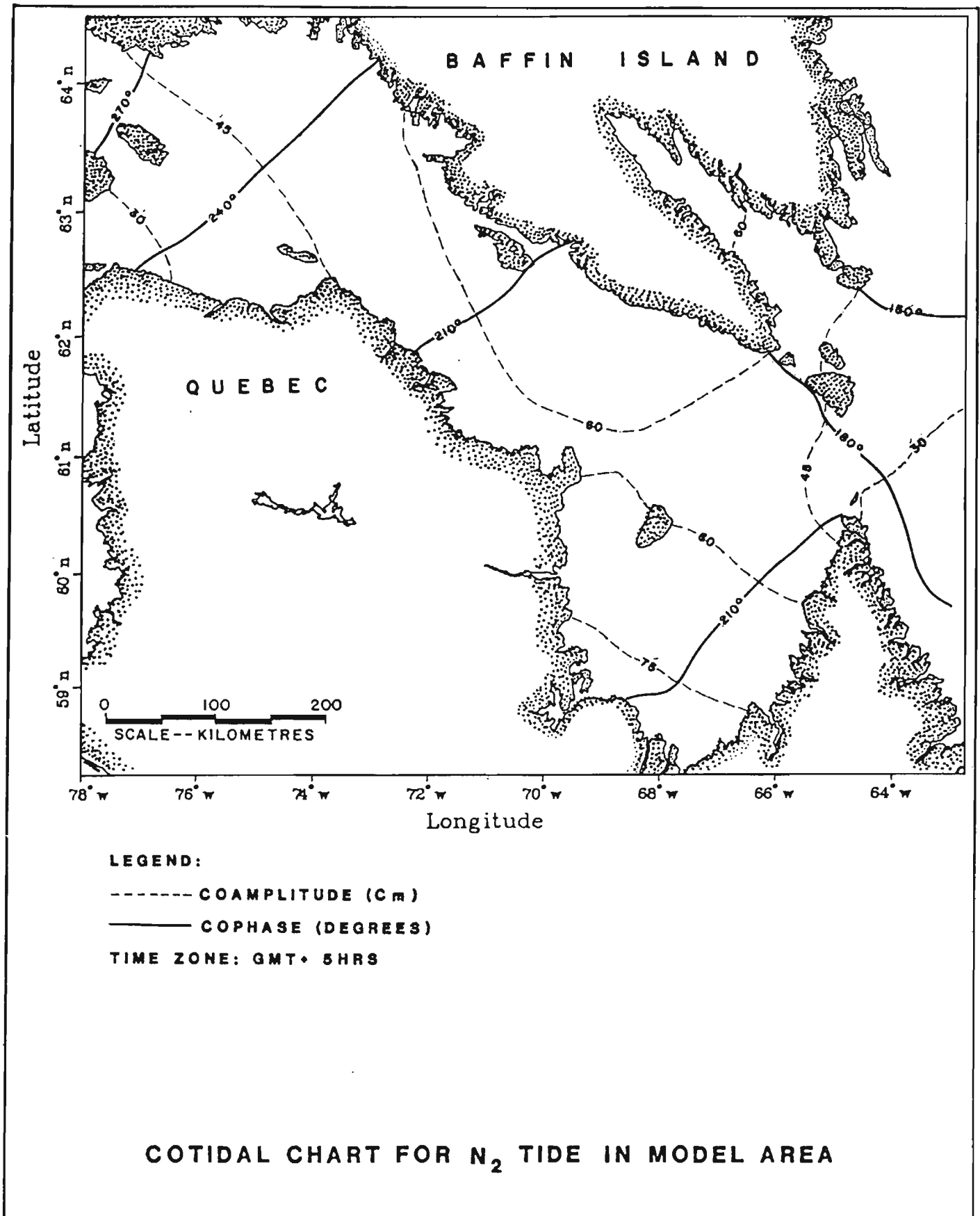


FIGURE 8

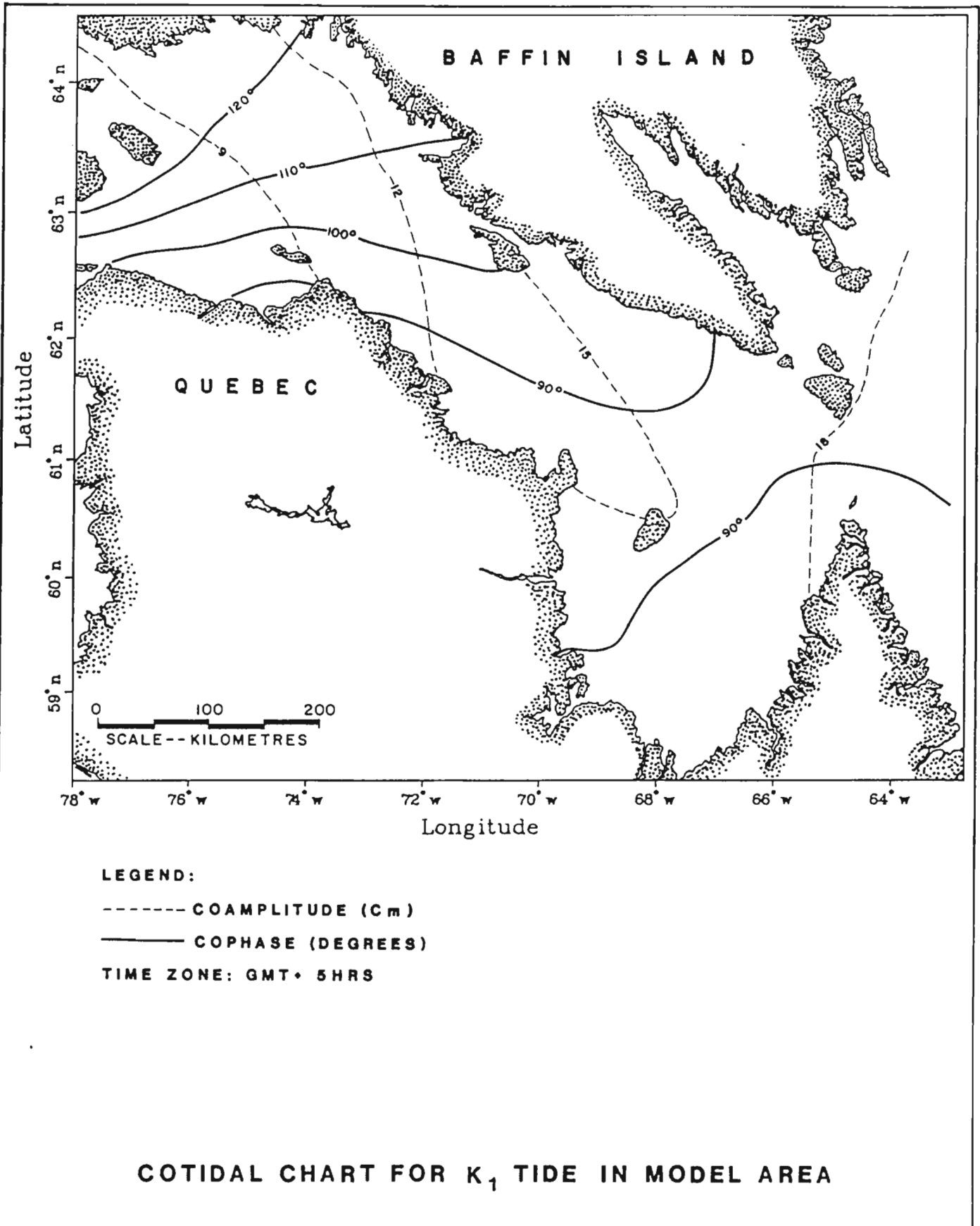


FIGURE 9

four modelled constituents and show the amplitude contours (in cm) and the cophase lines (in degrees referred to Greenwich Mean Time plus 5 hours).

For the  $M_2$  tide the agreement with the reference stations is good, the largest difference being a 5.2% overestimate in amplitude at Doctor Island and a  $13^\circ$  phase lead at Acadia Cove. It can be noted, however, that for these stations the cotidal charts (Godin, 1980 and Dohler, 1966) support the model results rather than the observations. As stated previously the data collected at Acadia Cove may be affected by the dynamic tidal activity at the entrance to Hudson Strait. Since at present there is no way to ascertain whether these observations are in error, we shall assume that they are correct and we shall take the difference between them and model results as the worst expected errors. For the  $M_2$  amplitude the standard deviation for the reference stations is 2.1% and should be representative of typical expected accuracy. The accuracy of model results, in terms of percentage, for the other constituents is somewhat lower than the  $M_2$ , however, since they have a smaller absolute magnitude their effect on tidal prediction is diminished.

When comparing the model results to all available tidal observations (see Appendix I), we find that five stations are systematically wrong (Stations 8, 12, 13, 14, and 17 shown in Table 1 and Figure 2). With the exception of Station 12, these are all located 12 to 15 km upstream of river mouths, in estuaries too small to be resolved by the model. These observations are therefore not representative of the coastal tides and will not be considered further. Smaller models with higher resolution will be needed to correctly predict the water levels in upstream regions of long inlets and estuaries. Station 12 was dismissed as being erroneous since it shows inexplicable differences with nearby Diana Bay which is the principal tidal station in the study area.

Considering all remaining observations, we find that the accuracy for the amplitude of the  $M_2$  tide is generally better than  $\pm 4\%$  or  $\pm 8$  cm, while the phase agreements are better than  $13^\circ$  or 26 minutes. For the other constituents the percent amplitude difference tends to be higher; however, because the constituents themselves are smaller, the absolute error is still in the order of  $\pm 6$  cm for each constituent. The maximum cumulative error in predicted water level, obtained by adding the  $M_2$ ,  $S_2$ ,  $N_2$  and  $K_1$  constituents is 31 cm or 2.6% of the tidal range, and occurs at Ashe Inlet. At other stations the error averages  $\pm 8$  cm.

#### 4.2 Tidal Currents

The barotropic tidal model generates current information at each grid element for each of the modelled constituents. The tidal regime of the Hudson Strait/Ungava Bay area is dominated by the  $M_2$  semidiurnal constituent and as such the overall tidal flow can be represented in terms of the  $M_2$  tide. Extending the model simulation over several tidal cycles allows the non-linear effects of the tidal signal to be included in terms of residual flow and higher harmonics. Figures 10 to 21 show current vectors within the study area for each lunar hour of an  $M_2$  tidal cycle. For most navigational purposes the lunar hour can be considered equivalent to a standard hour (i.e. 60 minutes). The charts depict currents within the system that are due entirely to  $M_2$  tidal forcing and consequently do not include the effects of strong winds and other exceptional meteorological phenomena causing currents of a non-periodic nature. A separate allowance must also be made where the tidal flow conditions are significantly altered by local influences such as river discharge.

To promote clarity in the charts current vectors are displayed for only one out of two model grid elements. This series of current vector charts provides both a temporal and spatial description of the relative strength of the water flow within the Hudson Strait/Ungava Bay study area.

TIDAL CURRENTS  
HUDSON STRAIT, UNGAVA BAY AND APPROACHES

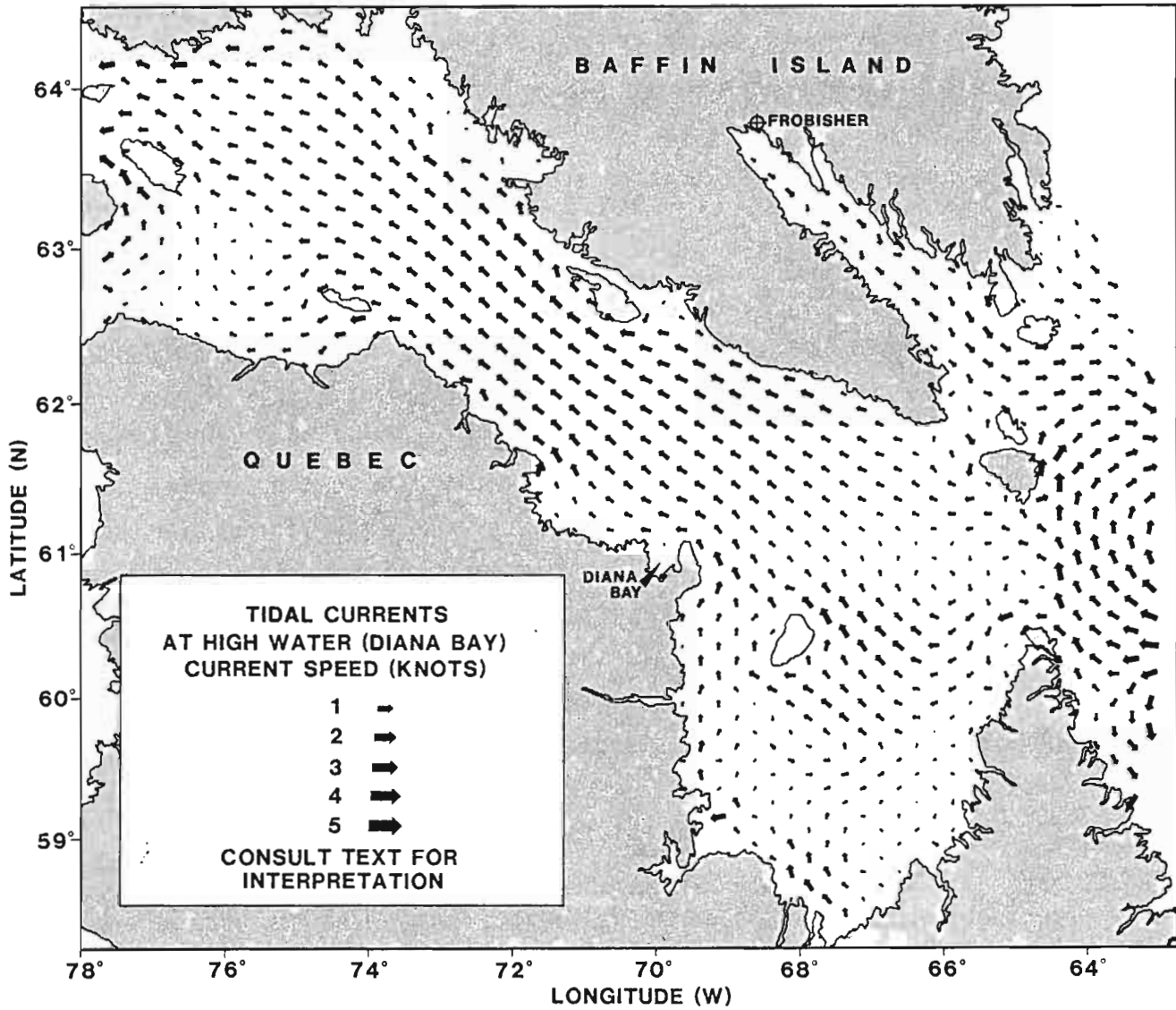


FIGURE 10



TIDAL CURRENTS  
HUDSON STRAIT, UNGAVA BAY AND APPROACHES

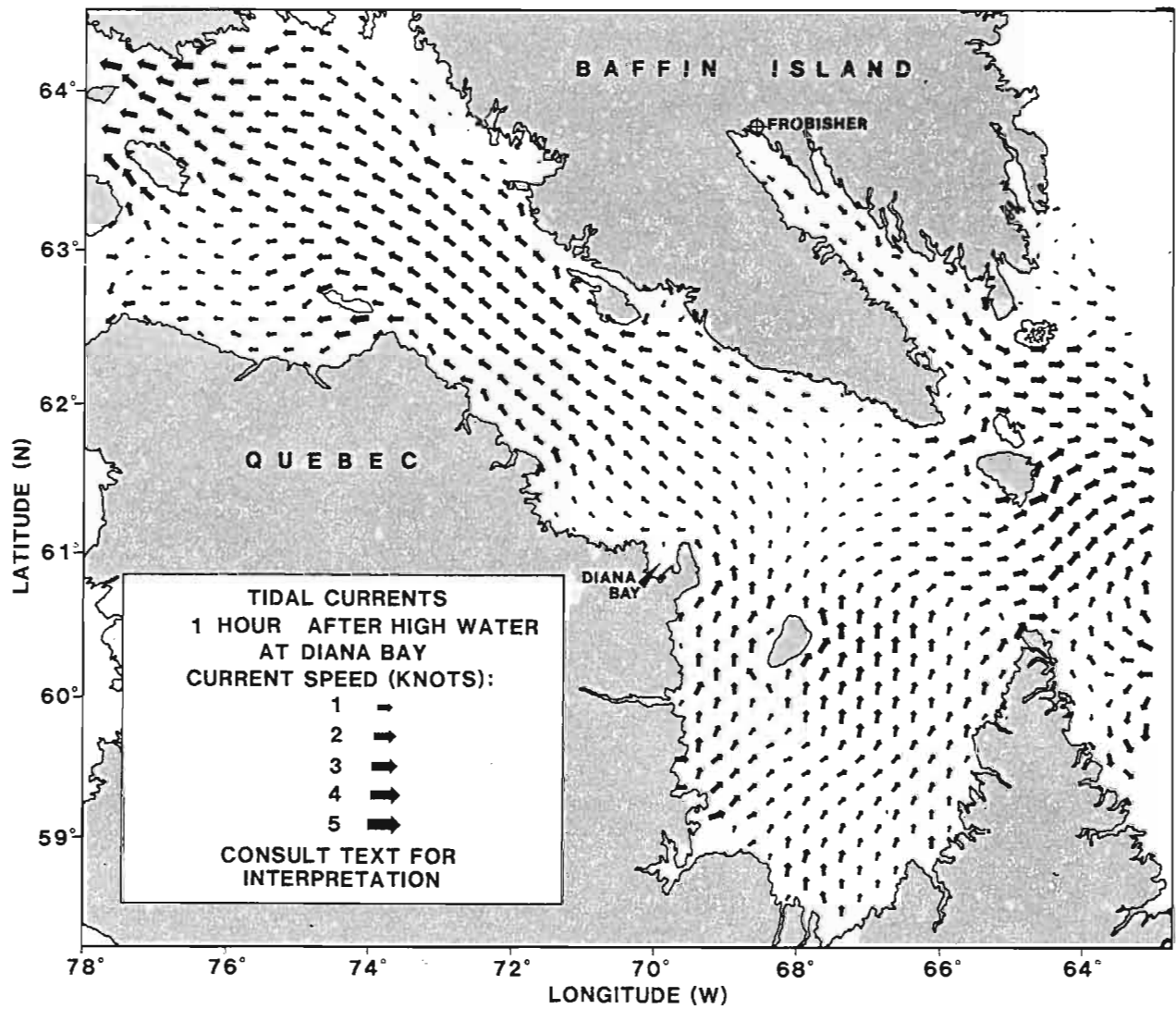


FIGURE 11

TIDAL CURRENTS  
HUDSON STRAIT, UNGAVA BAY AND APPROACHES

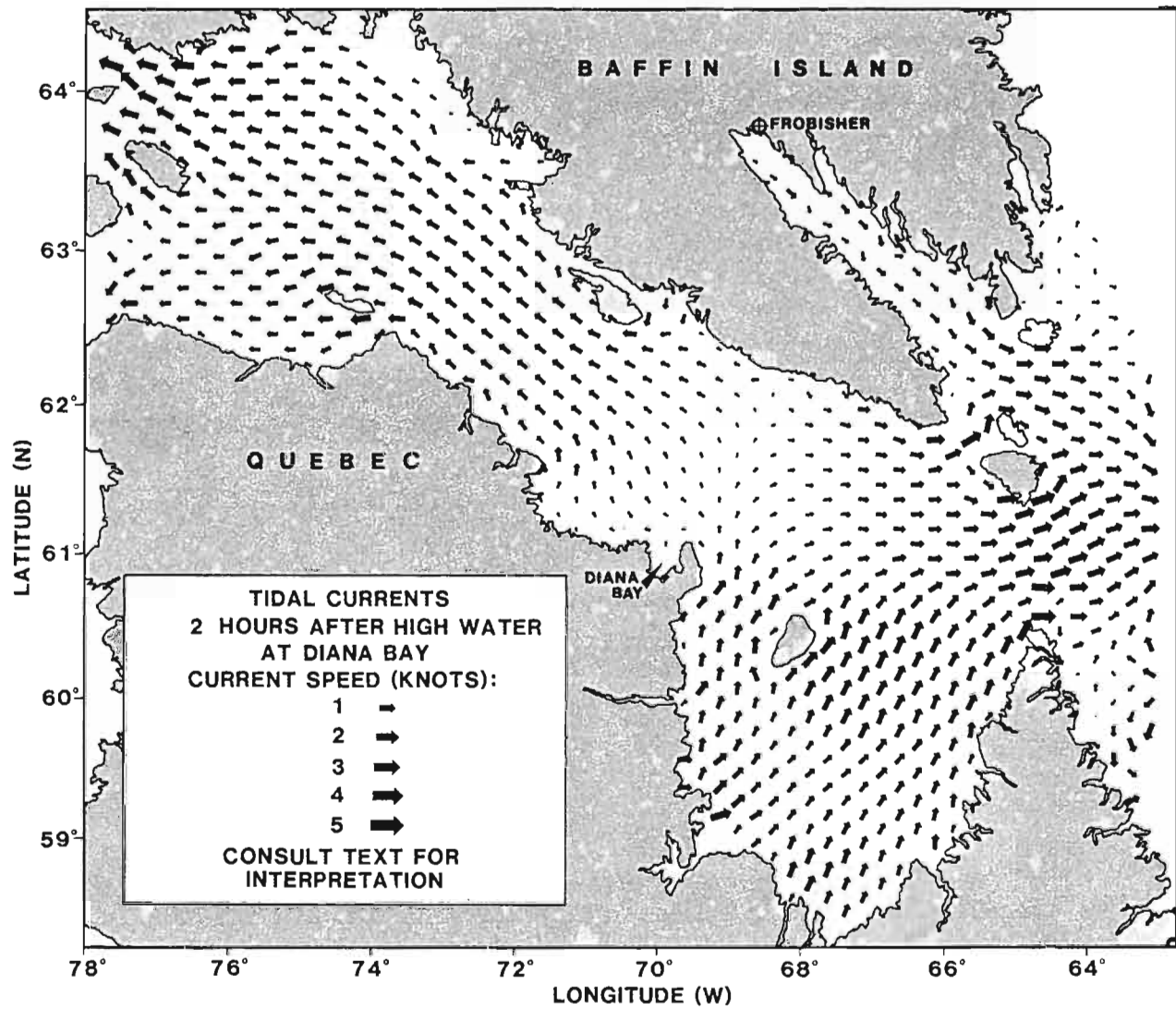


FIGURE 12

TIDAL CURRENTS  
HUDSON STRAIT, UNGAVA BAY AND APPROACHES

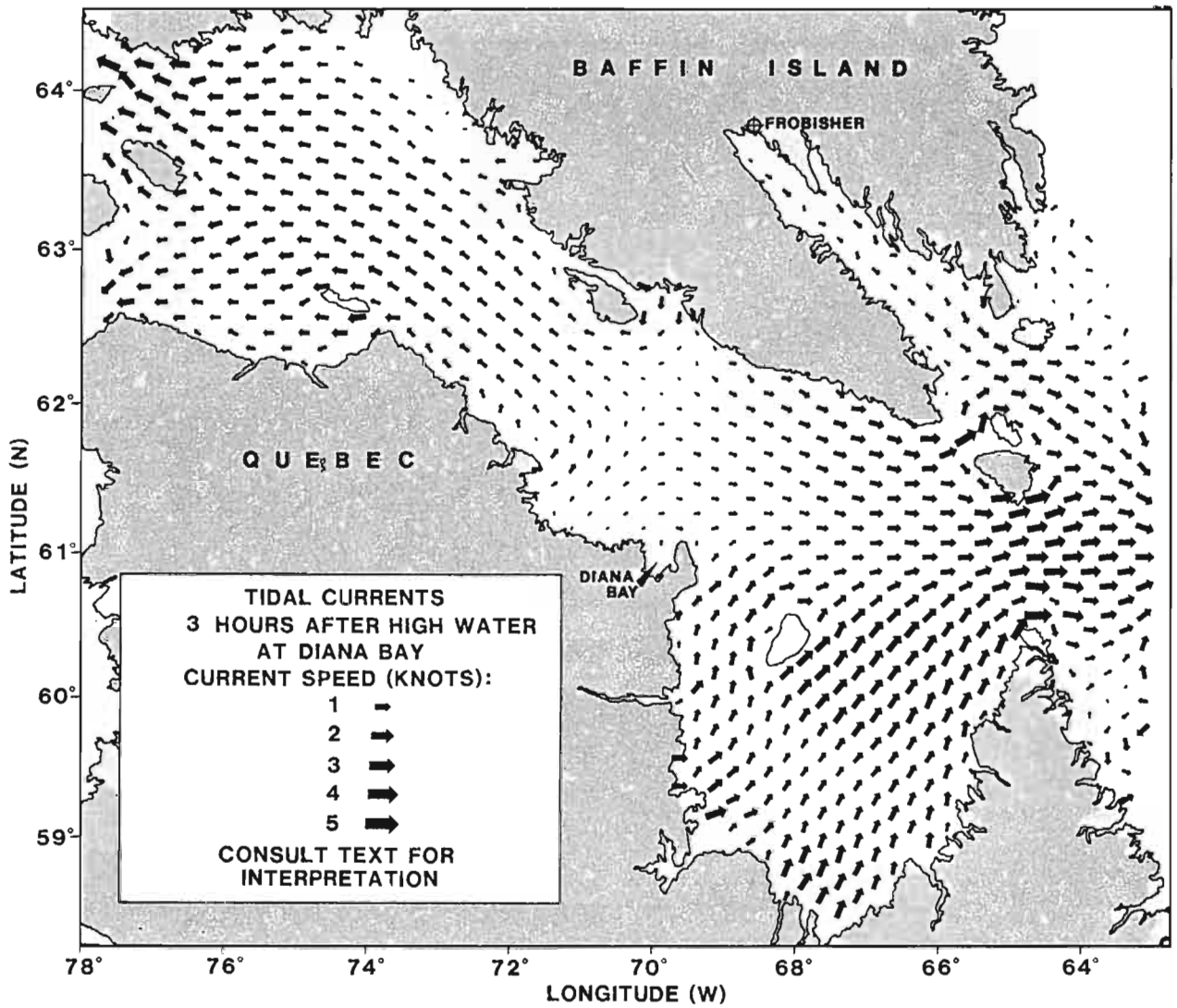


FIGURE 13

TIDAL CURRENTS  
HUDSON STRAIT, UNGAVA BAY AND APPROACHES

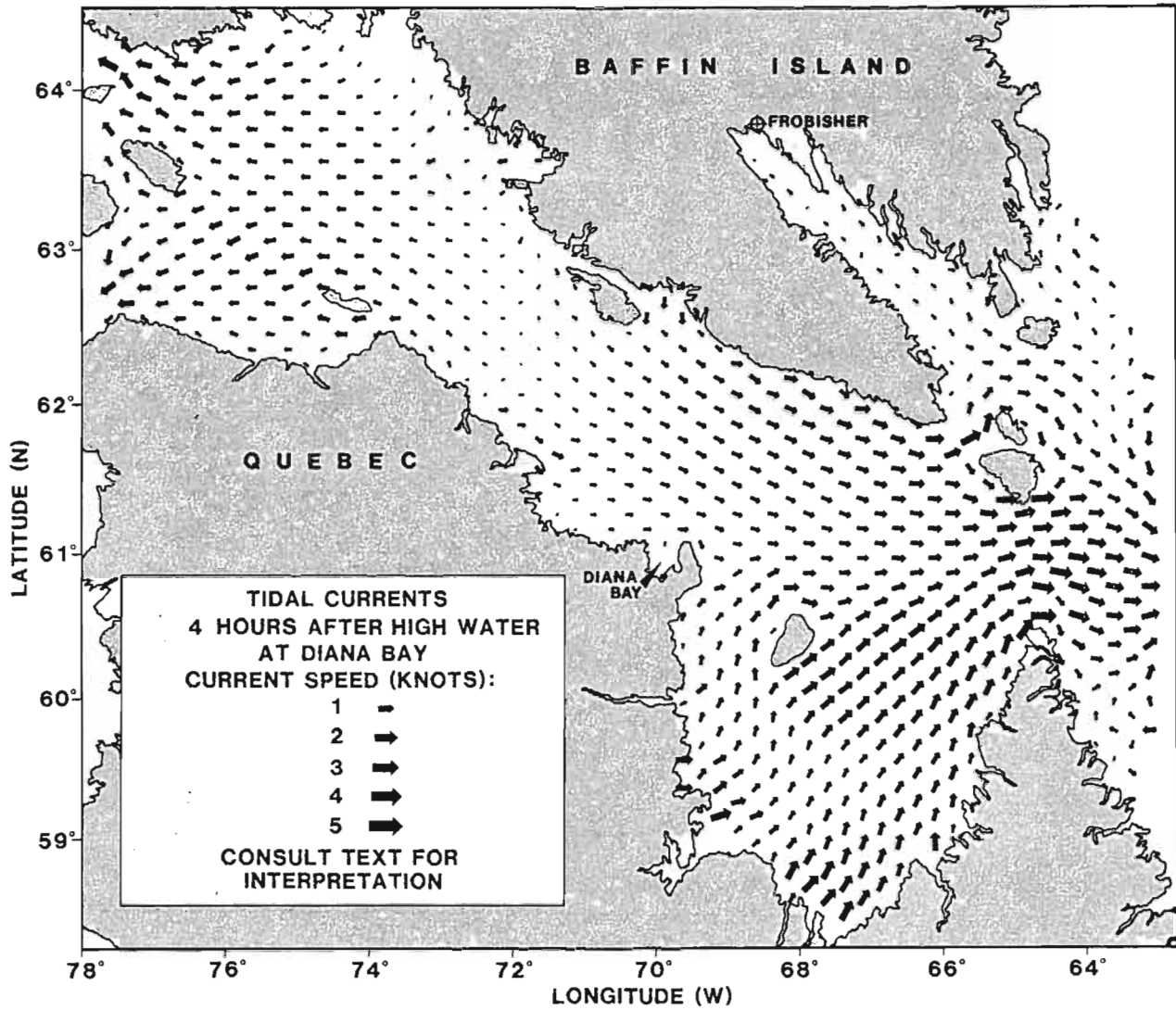


FIGURE 14

**TIDAL CURRENTS  
HUDSON STRAIT, UNGAVA BAY AND APPROACHES**

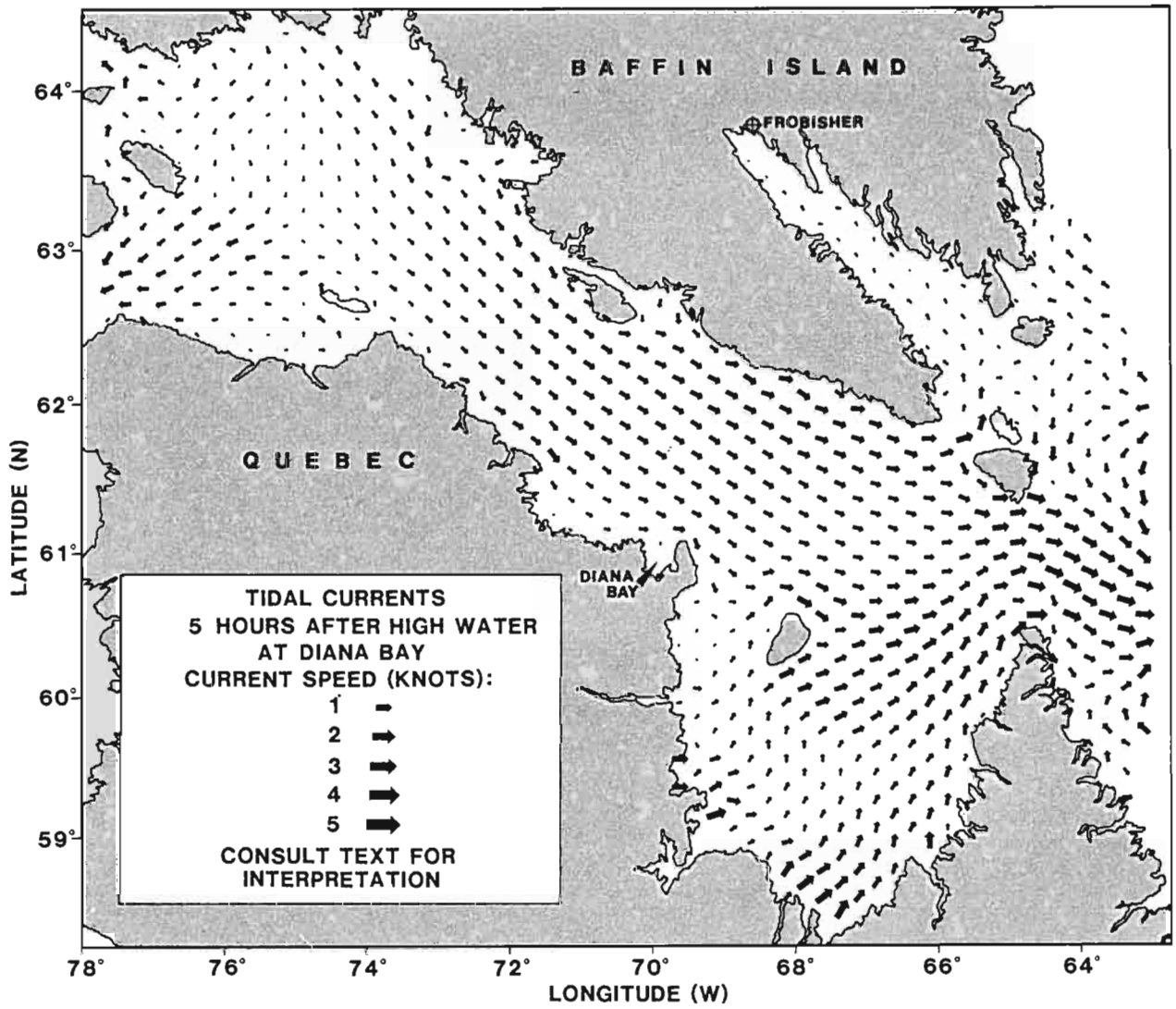


FIGURE 15

TIDAL CURRENTS  
HUDSON STRAIT, UNGAVA BAY AND APPROACHES

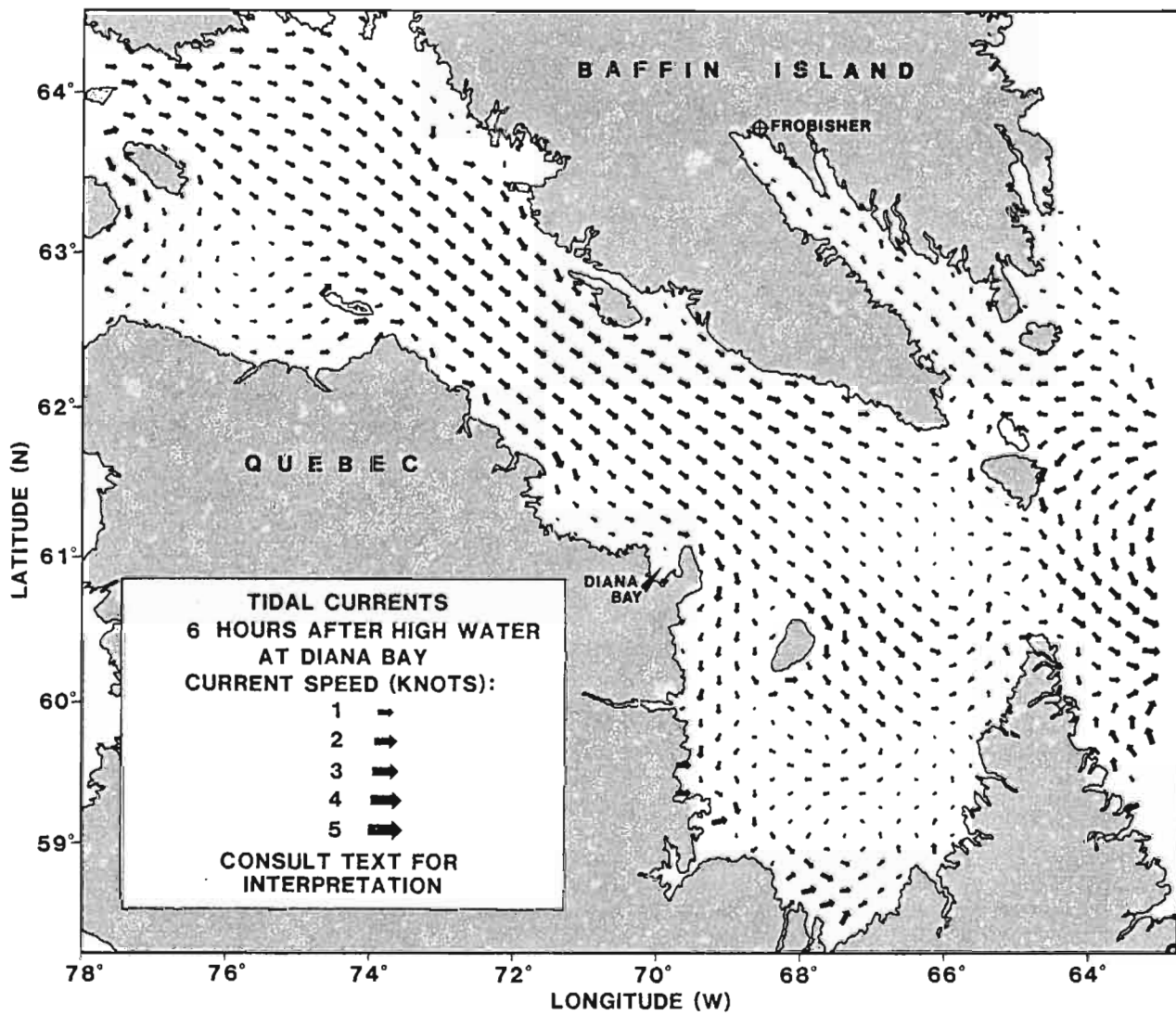


FIGURE 16

**TIDAL CURRENTS  
HUDSON STRAIT, UNGAVA BAY AND APPROACHES**

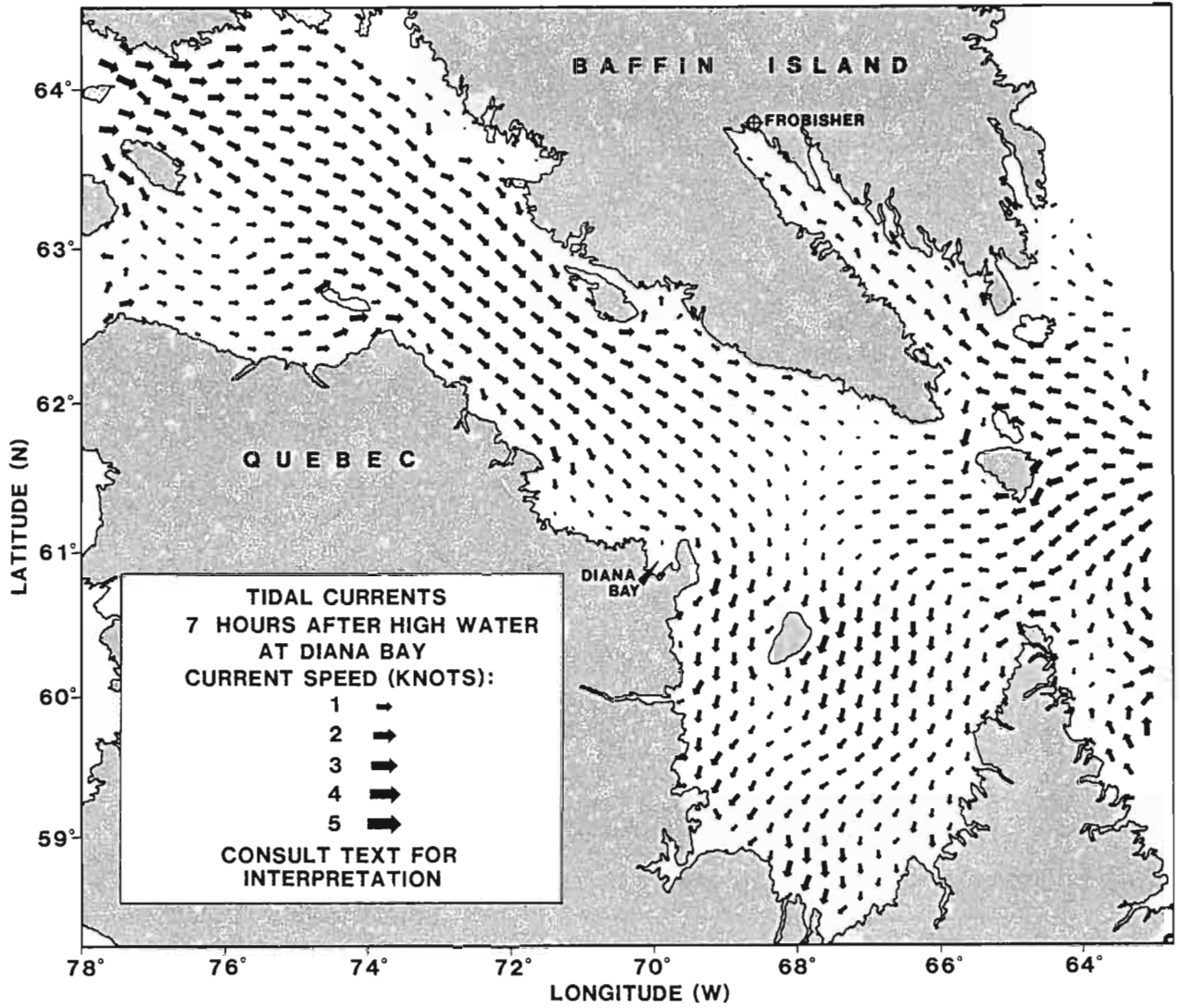


FIGURE 17

### TIDAL CURRENTS HUDSON STRAIT, UNGAVA BAY AND APPROACHES

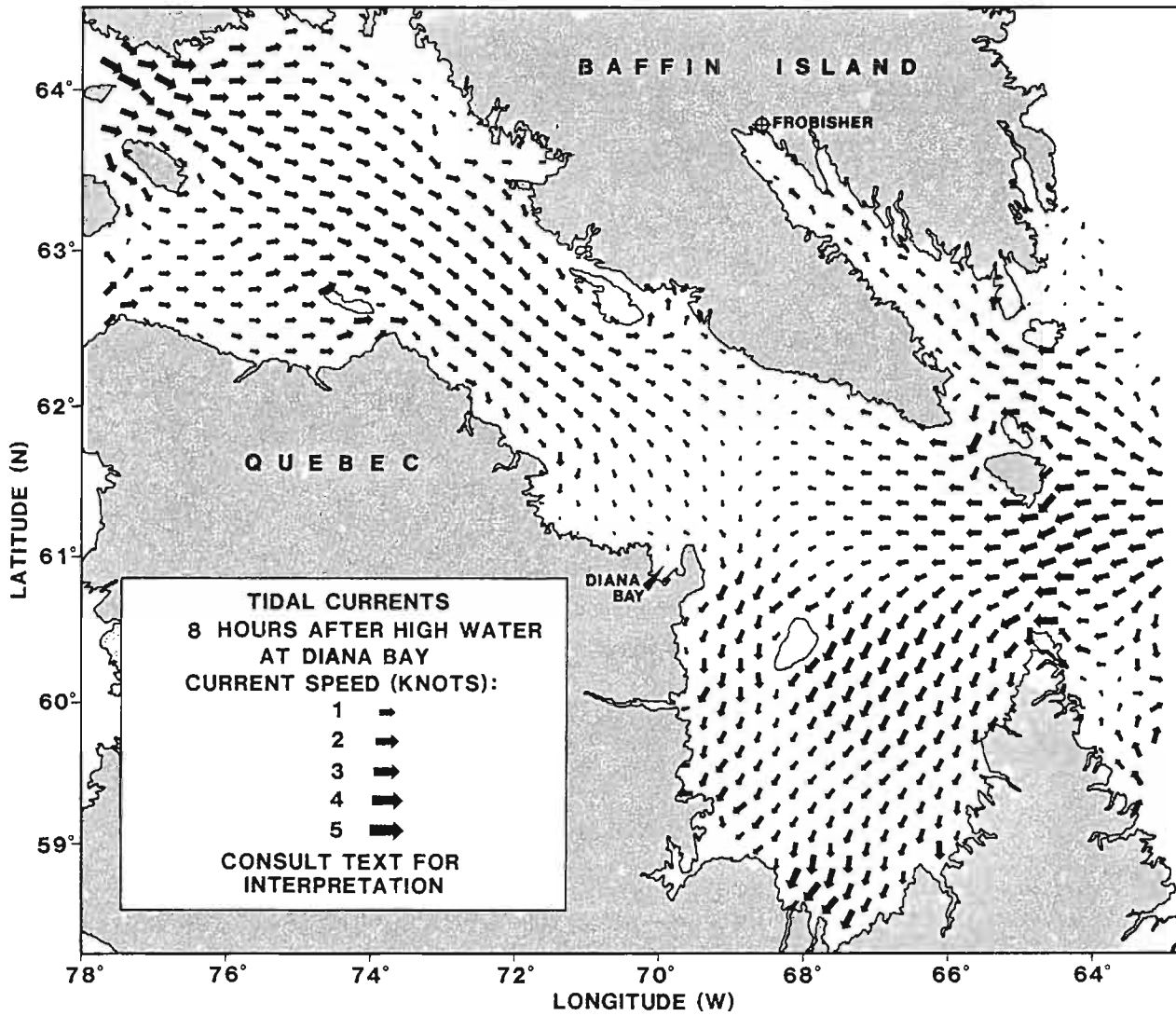


FIGURE 18



### TIDAL CURRENTS HUDSON STRAIT, UNGAVA BAY AND APPROACHES

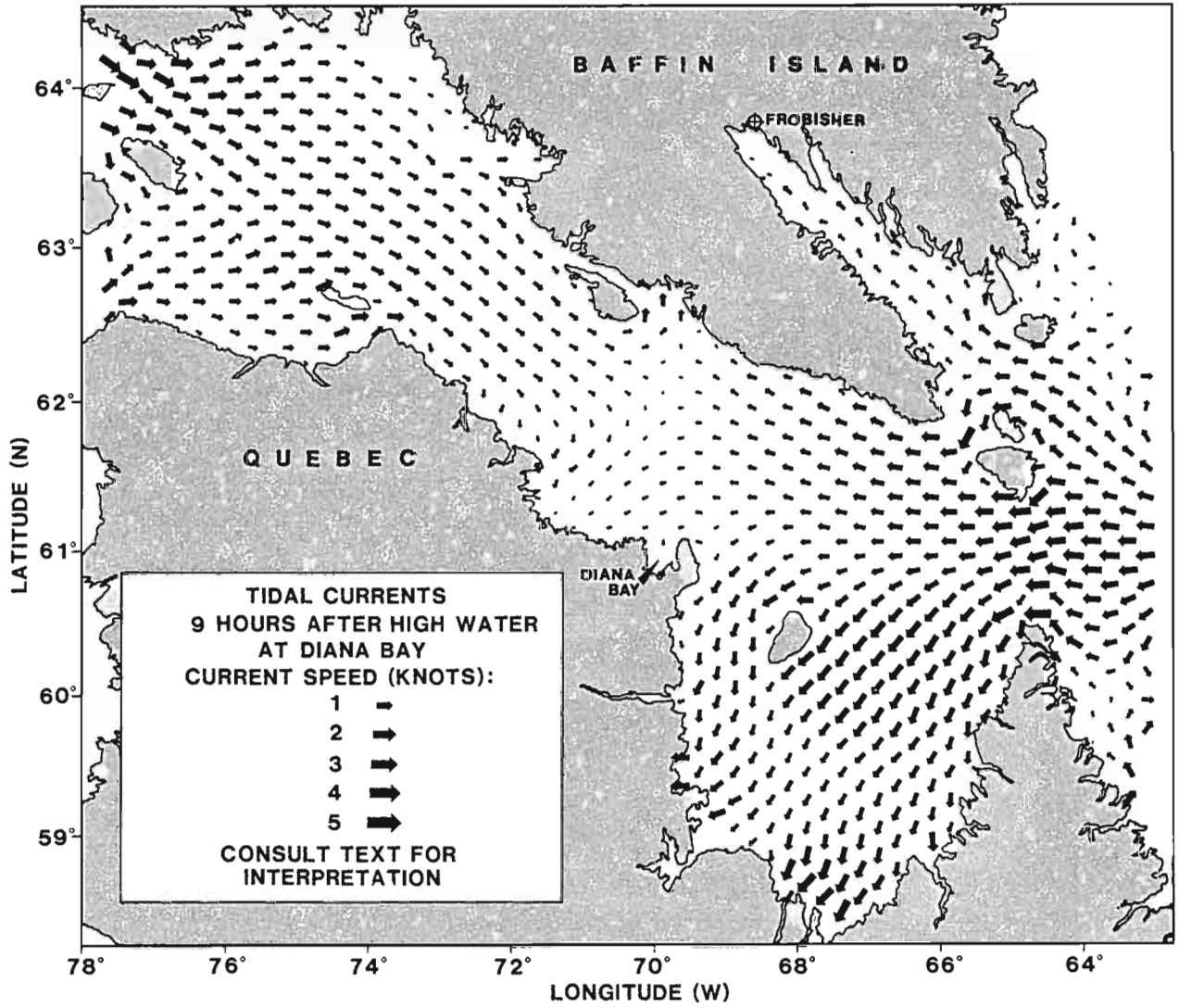


FIGURE 19

**TIDAL CURRENTS  
HUDSON STRAIT, UNGAVA BAY AND APPROACHES**

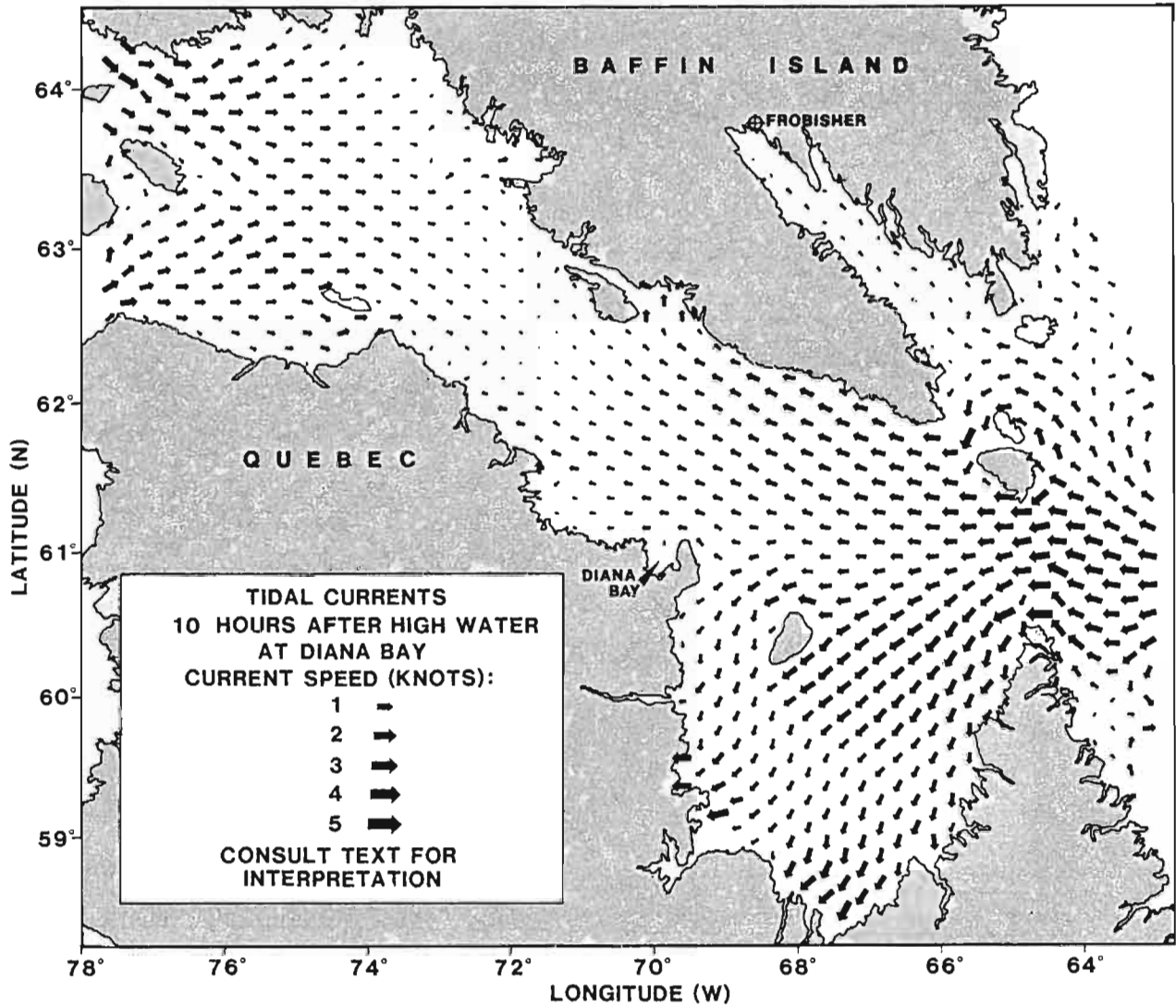


FIGURE 20

### TIDAL CURRENTS HUDSON STRAIT, UNGAVA BAY AND APPROACHES

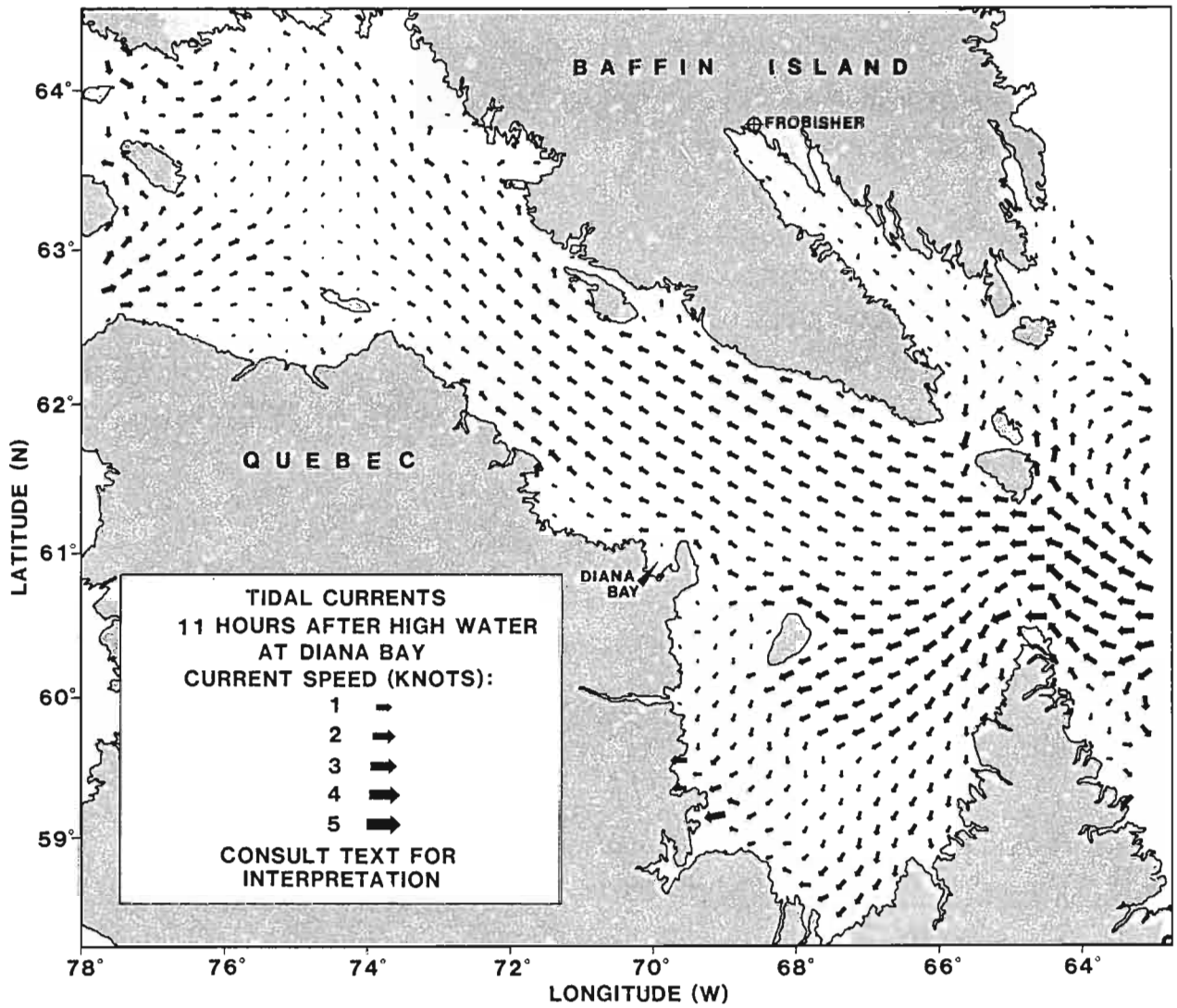


FIGURE 21

Being the principal tidal reference port in the study area Diana Bay, located near the midpoint of the Hudson Strait, was chosen as the reference location for the current vector charts. The timing of the currents is related to the time at which high water occurs at Diana Bay during Eastern Standard Time (available from the Canadian Hydrographic Service tide tables). When daylight saving time is in effect an extra hour must be added to the Diana Bay time. Care therefore should be taken to apply appropriate time corrections when operating in a time zone other than Eastern Standard Time. The currents shown are those to be expected for the mean tidal range of 6.4 m at Diana Bay. The following correction factors must be applied to the current speeds given in the vector diagrams to correspond to the actual tidal range at Diana Bay (also given in the tide tables) which varies due to the spring-neap cycle of the tide.

Correction Factors

<u>Range at Diana Bay</u>	<u>Multiply Current by</u>
5.5 m	0.9
6.5 m	1.0
7.5 m	1.2
8.5 m	1.3
9.5 m	1.5

Continuity arguments can be used to show that tidal currents and tidal elevation are directly related. It can be expected, therefore, that the accuracy of the modelled currents will reflect the accuracy of the previously examined water elevation (i.e. on the order of 2 to 5 percent). The modelled currents, however, represent a depth averaged velocity and as such do not include internal motions which may result in one layer of water sliding over another, at a different speed and, perhaps, in a different direction. Analysis of observed current behaviour provides the best means to assess the significance of these effects.

Quantitative tidal current measurements in the Hudson Strait/Ungava Bay area are sparse. The observations of Farquharson (1959) and Drinkwater (1983) do allow an examination of the vertical structure and tidal

components of flow at several locations within the study area. Table 5 summarizes the results of these observations and compares them to the currents numerically generated at corresponding grid elements in the model. As can be seen the observed tidal currents are nearly uniform with depth implying that shearing effects, if any, are weak. The representation of the current flow by the two-dimensional barotropic model should, therefore, be applicable.

The agreement between the observed tidal current and the numerically modelled tidal flow can be quantified by examining the root mean square (RMS) deviation of the modelled current from the observed current. This RMS deviation between observations and model results is  $\pm 0.06$  knots while the maximum difference is 0.23 knots. For navigational purposes it is often more useful to compare observed near surface currents with model results. In this case we find a maximum difference of .31 knots and an RMS deviation of  $\pm 0.09$  knots. In comparison to these differences it can be shown through the examination of Farquharson's (1959) data that observed differences between two time series of current speed recorded at the same location can be up to 0.35 knots, with discrepancies of  $\pm 0.10$  knots common. Keeping the accuracy of observations in mind it may be concluded that the model differences between modelled and observed currents may be attributed principally to observational uncertainties.

#### 4.3 Tidal Ellipses

Tidal flow patterns in Ungava Bay and Hudson Strait are presented in the form of tidal ellipses for the  $M_2$ ,  $N_2$ ,  $S_2$ , and  $K_1$  constituents in Figures 22 to 25. The tidal ellipses shown represent the path followed by water particles as they are carried by tidal currents. For clarity of presentation the ellipses in the figures are increased in scale by a factor of 2, 4, 4, and 8 for the  $M_2$ ,  $N_2$ ,  $S_2$ , and  $K_1$  components, respectively (e.g. the size of the  $M_2$  ellipse corresponds to twice the actual  $M_2$  tidal excursion at that location). An arrow head on each ellipse

TABLE 5. COMPARISON OF PREDICTED AND OBSERVED TIDAL FLOWS

Observation by Farquharson (1959)

Depth (m)	M <sub>2</sub> Major Axis			S <sub>2</sub> Major Axis			K <sub>1</sub> Major Axis		
	Direction (° True)	Amplitude (knots)	Phase (°GMT+5)	Direction (° True)	Amplitude (knots)	Phase (°GMT+5)	Direction (° True)	Amplitude (knots)	Phase (°GMT+5)
STATION A									
7	334	.96	275	334	.33	333	334	.12	148
20	332	.84	264	332	.29	322	332	.11	163
30	344	1.06	258	344	.37	316	344	.09	167
50	338	.56	267	338	.20	325	338	.06	155
Depth Average Observations	337	.72	273	338	.25	320	336	.07	150
Model Results	312	.85	279	310	.27	297	308	.05	146
STATION B									
7	305	1.14	273	305	.32	332	305	.08	185
20	312	1.12	271	313	.91	330	312	.12	165
30	315	1.11	263	315	.31	322	315	.09	155
50	303	.69	254	303	.19	315	303	.10	43
75	307	.56	248	307	.16	309	307	.08	333
100	309	.52	248	309	.15	309	309	.08	240
150	307	.55	253	307	.15	314	307	.06	277
230	311	.33	241	311	.09	302	311	.09	13
Depth Average Observations	309	.60	257	310	.21	318	306	.02	309
Model Results	321	.83	279	308	.27	297	306	.05	150

TABLE 5. continued

Observation by Farquharson (1959)

Depth (m)	M <sub>2</sub> Major Axis			S <sub>2</sub> Major Axis			K <sub>1</sub> Major Axis		
	Direction (° True)	Amplitude (knots)	Phase (°GMT+5)	Direction (° True)	Amplitude (knots)	Phase (°GMT+5)	Direction (° True)	Amplitude (knots)	Phase (°GMT+5)
STATION C									
7	310	1.11	255	310	.40	305	310	.07	122
30	305	1.07	266	305	.39	316	305	.09	153
50	296	.85	269	296	.31	319	296	.02	345
100	302	.81	270	302	.29	320	302	.04	84
150	299	.94	263	299	.34	313	-	-	-
200	310	.83	285	310	.30	335	310	.09	138
300	307	.81	246	307	.30	356	-	-	-
Depth Average									
Observations	305	.84	266	304	.31	316	308	.06	130
Model Results	308	.84	260	307	.28	297	307	.06	152
STATION D									
7	280	.85	291	280	.20	328	280	.15	181
20	289	.91	293	289	.22	330	289	.17	148
30	276	.88	284	276	.21	321	276	.08	153
50	297	.92	267	297	.22	306	297	.05	223
100	300	1.08	266	300	.26	305	300	.11	178
150	307	1.08	263	307	.26	302	307	.04	123
200	300	.95	267	300	.23	302	300	.03	270
300	316	.72	243	316	.17	282	316	.03	202
Depth Average									
Observations	303	.88	263	302	.20	302	299	.03	217
Model Results	307	.92	282	306	.30	296	306	.06	153

TABLE 5. continued

Observation by Farquharson (1959)

Depth (m)	M <sub>2</sub> Major Axis			S <sub>2</sub> Major Axis			K <sub>1</sub> Major Axis		
	Direction (° True)	Amplitude (knots)	Phase (°GMT+5)	Direction (° True)	Amplitude (knots)	Phase (°GMT+5)	Direction (° True)	Amplitude (knots)	Phase (°GMT+5)
STATION E									
7	311	1.10	250	311	.30	311	311	.10	101
20	298	1.13	257	298	.31	318	298	.06	274
30	290	1.13	267	290	.31	328	290	.07	284
50	291	.90	267	291	.25	328	291	.07	289
100	292	1.01	264	292	.28	325	292	.04	97
100	299	1.08	262	299	.30	323	299	.07	147
200	308	1.01	258	308	.28	319	308	.10	140
300	322	.69	237	322	.19	298	322	.05	177
Depth Average Observations	304	.89	256	304	.25	317	305	.06	154
Model Results	307	.99	283	306	.33	295	306	.06	153
STATION F									
7	265	1.07	271	265	.34	328	265	.06	248
20	270	1.14	264	270	.36	321	-	.00	-
30	269	1.20	263	269	.38	320	269	.08	178
50	280	.98	261	280	.32	318	-	.00	-
100	287	.98	260	287	.32	317	287	.07	113
150	276	1.12	258	276	.37	315	276	.11	134
200	286	1.18	261	286	.38	318	286	.09	124
290	276	1.06	241	276	.34	298	276	.08	127
Depth Average Observations	280	1.07	257	280	.35	313	278	.08	136
Model Results	310	1.11	288	310	.37	290	310	.07	144



TABLE 5. continued

## Observations by Drinkwater (1983)

Depth (m)	M <sub>2</sub> Major Axis			M <sub>2</sub> Minor Axis
	Direction (° True)	Amplitude (knots)	Phase (°GMT+5)	Amplitude (knots)
STATION HS1				
30	287	.58	224	.11
50	283	.57	224	.10
100	293	.58	221	.13
200	296	.46	215	.02
Depth Average				
Observations	292	.52	220	.08
Model Results	302	.54	209	.10
STATION HS2				
30	299	.40	215	.09
Depth Average				
Observations	299	.40	215	.09
Model Results	299	.62	192	.18
STATION HS3				
30	297	.50	202	.05
200	292	.54	207	.11
Depth Average				
Observations	294	.52	206	.09
Model Results	295	.69	183	.12
STATION HS4				
30	290	.91	205	.09
100	296	.81	199	.00
Depth Average				
Observations	293	.85	202	.05
Model Results	291	.85	186	.03
STATION HS5				
30	291	.76	144	.26
200	272	.57	162	.09
Depth Average				
Observations	283	.61	158	.14
Model Results	284	.69	159	.11

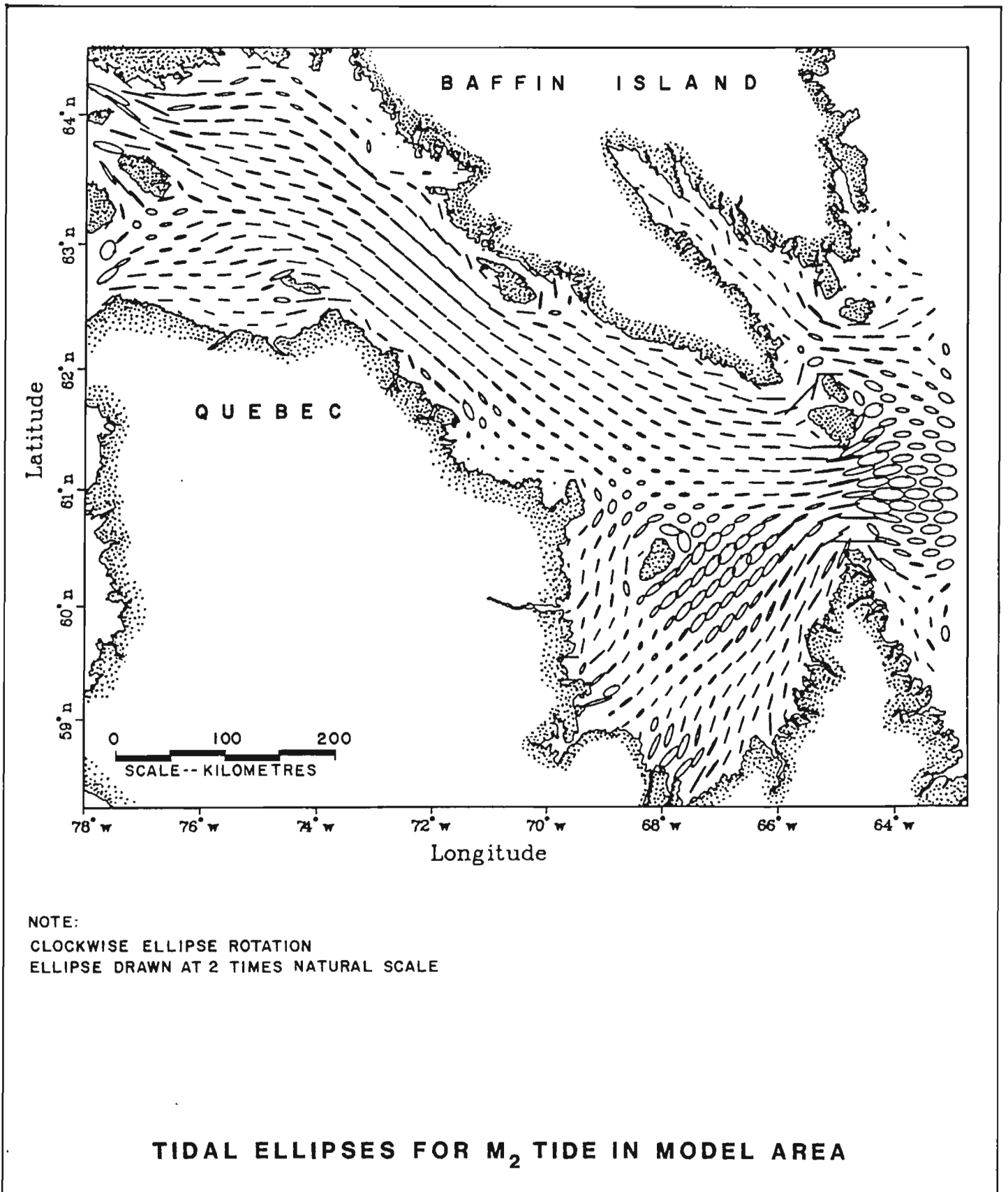


FIGURE 22

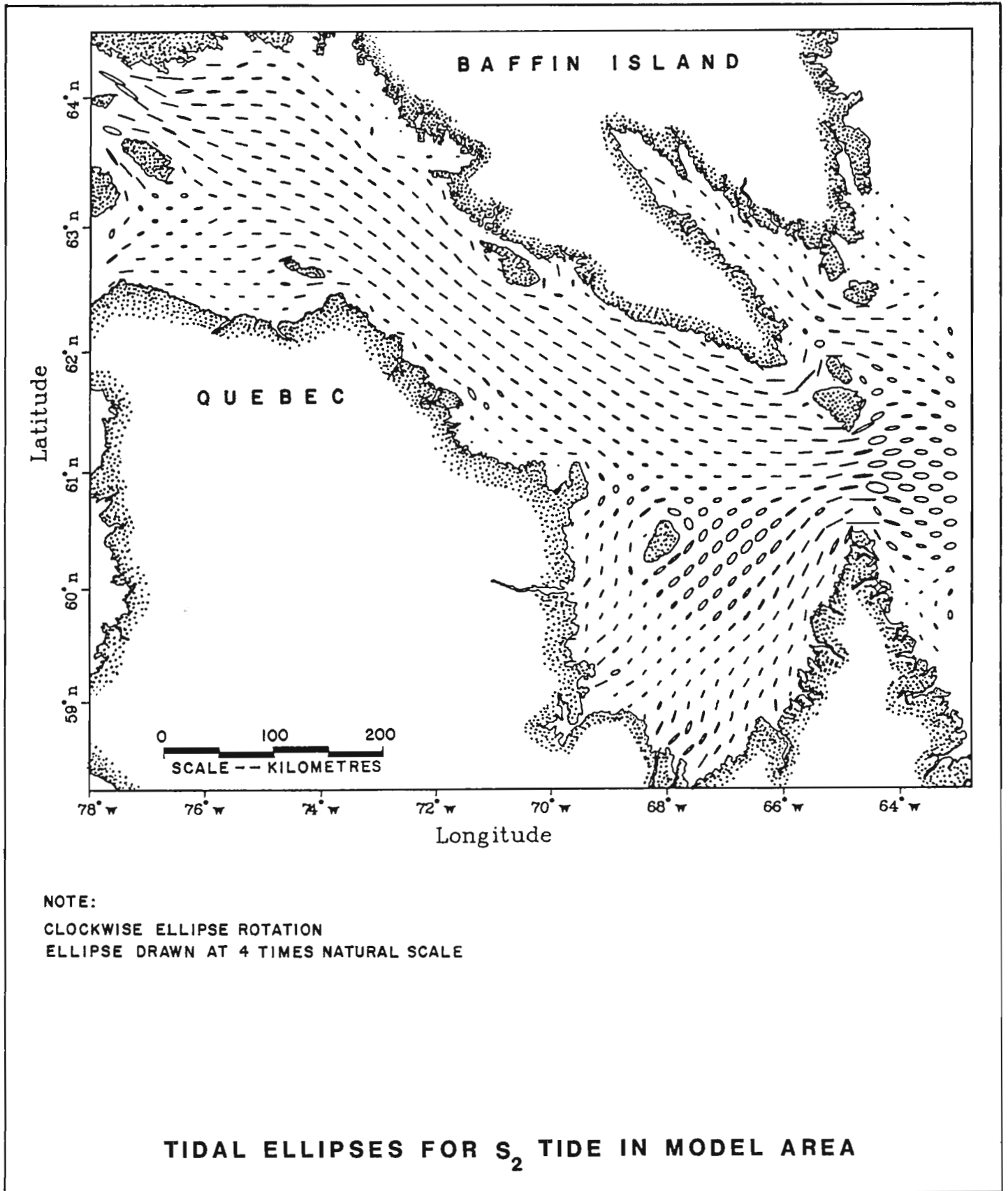


FIGURE 23

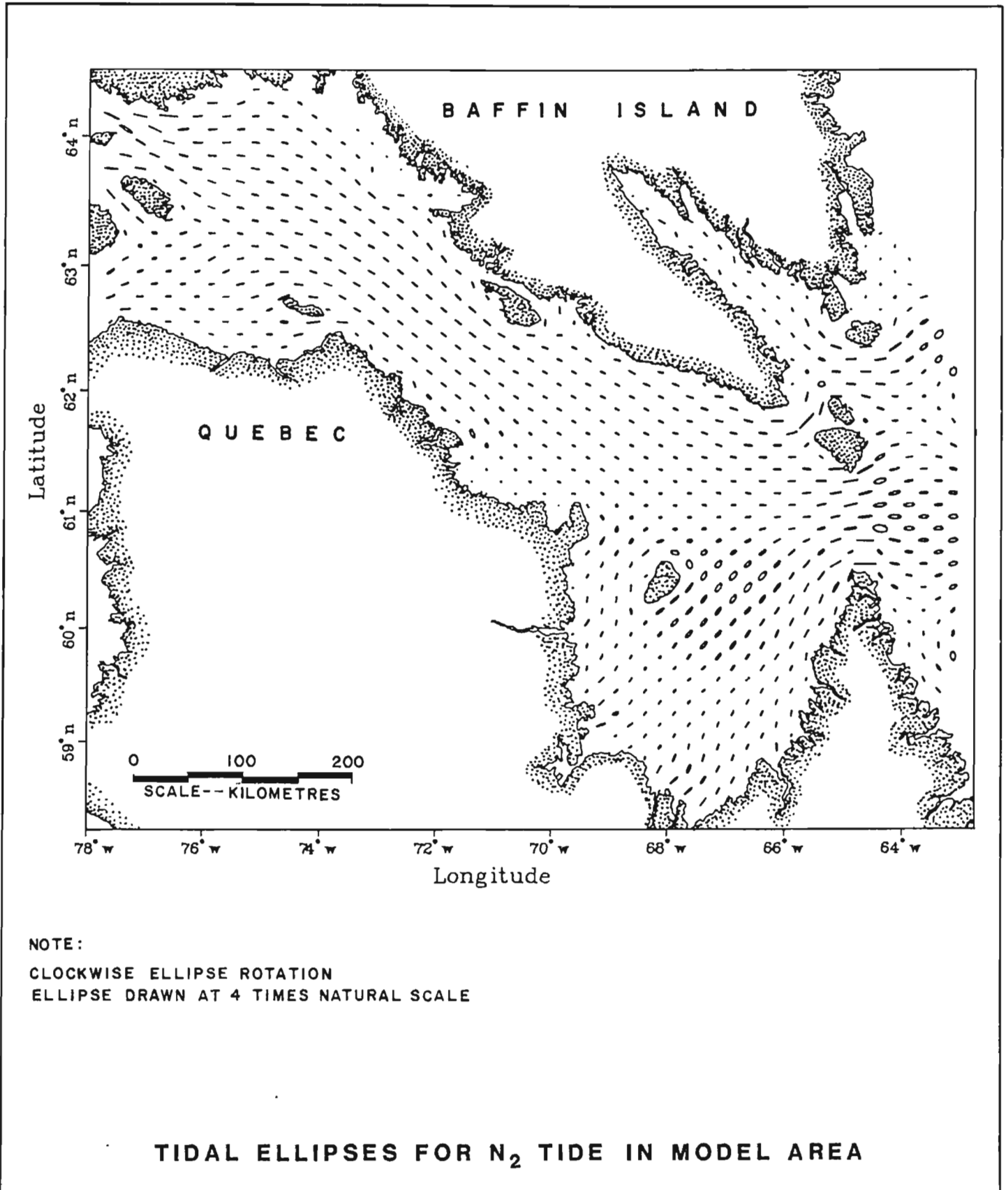


FIGURE 24

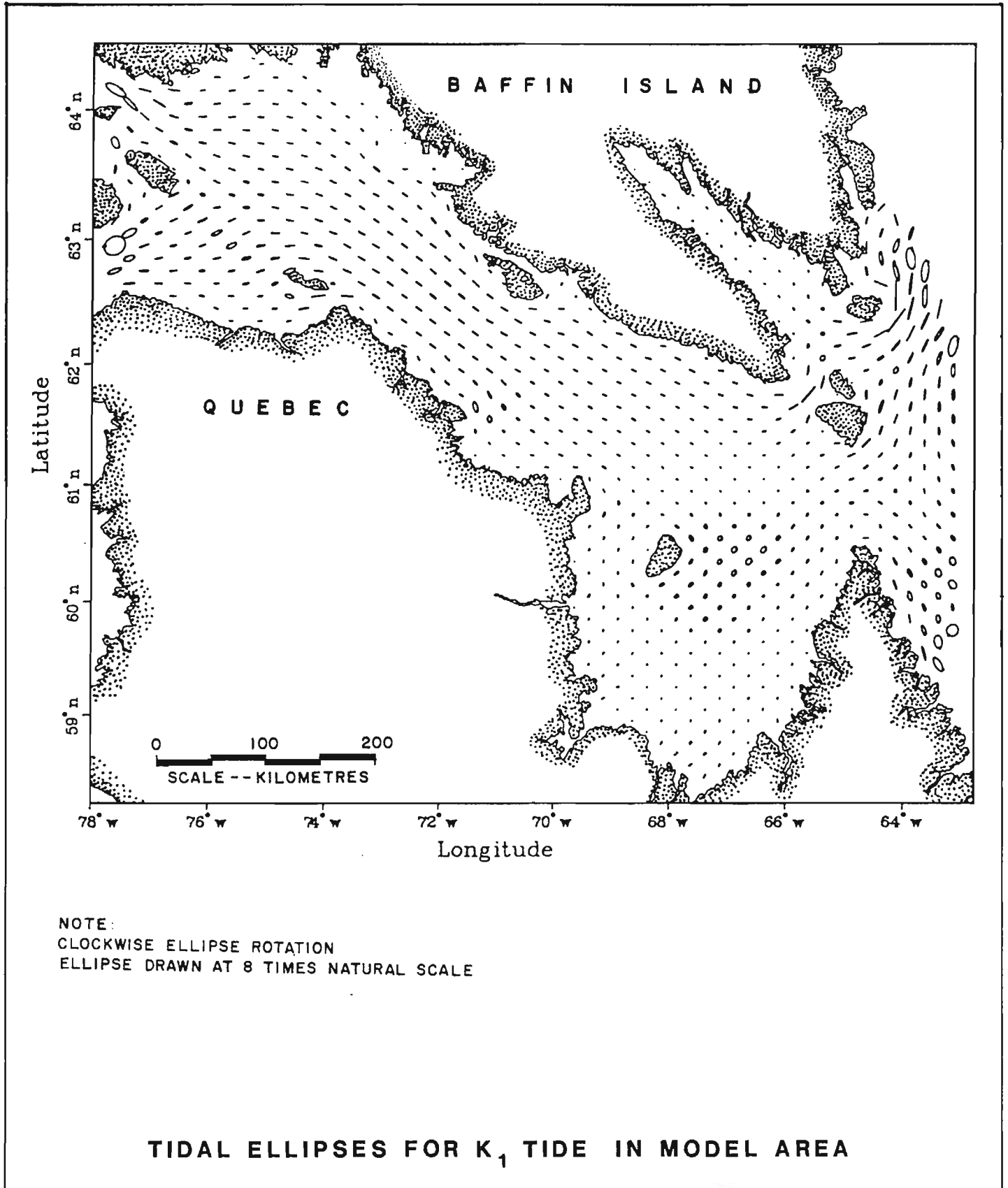


FIGURE 25

indicates the direction of travel of the water particle during the tidal cycle. Although these arrows are only visible on the larger ellipses their direction of rotation is clockwise throughout the study area.

From these plots the dominance of the  $M_2$  tide can again be identified. It can also be seen that tidal flow is rectilinear (i.e. consisting mainly of a back and forth motion) over most of the study area. A marked rotational character is evident only near open ocean boundaries and in the middle of Ungava Bay where the water flow is less constrained by the presence of land.

#### 4.4 Sensitivity of Model Bathymetry

As discussed in Section 3.1 the input bathymetric data file for the study area was supplemented in several areas for which no depth measurements were available. A linear bottom slope was assumed for those regions at which estimated bathymetric values were necessary. In order to assess the sensitivity of the numerical model to changes in the bathymetry input data, and hence determine the uncertainty in the model results, the  $M_2$  tide was simulated for two runs with modified bathymetry. The first sensitivity run doubled the estimated bathymetric values and the second run halved these values. Comparison of the model results indicated that the variation in bathymetry, i.e. the sensitivity of the model to bathymetric uncertainty, is less than five percent for amplitude and three percent for phase lag. The biggest changes occur at the head of Ungava Bay.

#### 4.5 Discussion

Numerically modelling the tidal regime in the Hudson Strait/Ungava Bay system has provided quantitative values that agree well with the available observed tidal information in the region. Comparison of observed and modelled tidal amplitudes show typical differences in the order of

2.1 percent and the expected accuracy of modelled tidal currents is at least as good as that from presently available data. It can be expected therefore that the model results are of comparable accuracy within the model domain allowing insight into the tidal characteristics throughout the study area. The charts of current strength and direction can be used to show mariners where and when to expect certain flow conditions which should be an advantage to the navigation of vessels of all sizes. The overall circulation patterns derived by the numerical model will contribute to the information required by scientists investigating the oceanographic processes that exist in the region. A broader understanding of the physical phenomena of water flow will be of benefit to engineering applications, such as the planning of harbours or determining the feasibility of tidal generation plants, and also to ecological concerns such as the distribution of larvae or fish populations.

It is considered that the limiting factor of accuracy in the numerically modelled results at this point can be attributed to the precision of the observed tidal data used to calibrate and validate the model. The model has been structured so that future observational information (such as bathymetry or tidal data) can be easily incorporated as input and consequently refine the present model results. Alternatively, the model area can be expanded to include new area to allow a more global perspective of tidal currents in Canada's arctic waterways.

5. REFERENCES

- Canadian Hydrographic Service. 1981. Atlas of Tidal Currents, Bay of Fundy and Gulf of Maine, 36 p.
- Canadian Hydrographic Service. 1983. Sailing Directions, Labrador and Hudson Bay, Fifth ed., 450 p.
- Canadian Hydrographic Service. 1984. Canadian Tide and Current Tables, Arctic and Hudson Bay, Vol. 4, 51 p.
- Dohler, G. 1966. Tides in Canadian Waters, Canadian Hydrographic Service, Marine Sciences Branch, Department of Mines and Technical Surveys, Ottawa, Ontario, 16 p.
- Drinkwater, K. 1983. Moored Current Meter Data from Hudson Strait, 1982, Canadian Data Report of Fisheries and Aquatic Sciences 381, Marine Ecology Laboratory, Ocean Science and Surveys, Atlantic Department of Fisheries and Oceans, Bedford Institute of Oceanography, Dartmouth, N.S.
- Easton, A.K. 1972. Tides of Hudson Strait, Bedford Institute of Oceanography, Report Series, BI-R-72-6.
- Farquharson, W.I. 1959. Tidal and Oceanographic Survey of Hudson Strait, August and September 1959, Canadian Hydrographic Service, Department of Mines and Technical Surveys, Ottawa, Ontario.
- Foreman, M.G.G. 1979. Manual for Tidal Heights: Analysis and Prediction, Pacific Marine Science Report 77-10, Reprinted with corrections. Institute of Ocean Sciences, Patricia Bay, Sidney, B.C., 97 p.
- Freeman, N.G. and T.S. Murty. 1976. Numerical Modelling of Tides in Hudson Bay, Journal of the Fisheries Research Board Canada, Vol. 33, pp. 2345-2361.
- Godin, G. 1980. Cotidal Charts for Canada, Marine Sciences and Information Directorate, Department of Fisheries and Oceans, Ottawa, Ontario, 93 p.
- Griffiths, D.K., R.D. Pingree and M. Sinclair. 1981. Summer Tidal Fronts in the Near-Arctic Regions of Foxe Basin and Hudson Bay, Deep Sea Research, Vol. 28A, No. 8, pp. 865-873.
- Martec Limited. 1983. Internal Wave Study. Prepared under contract 09SC.FP901-2-X035 for Department of Supply and Services, 57 p.
- Martec Limited. 1984a. Ungava Bay Tidal Elevation and Current Numerical Model Development. Prepared under Contract 10SC.FP901-3-R062 for Department of Supply and Services, 46 p.



Martec Limited. 1984b. User Manual for Barotropic Circulation Model. Prepared under contract 09SC.FP901-3-X064 for Department of Supply and Services, 29 p.

Schwiderski, E.W. 1980. On Charting Global Ocean Tides, Review of Geophysical Space Physics, Vol. 18, p. 243-268.

APPENDIX I

COMPARISON OF OBSERVED AND MODELLED TIDES  
IN HUDSON STRAIT/UNGAVA BAY

COMPARISON OF AMPLITUDES OF OBSERVED AND MODELLED TIDES (cm)

Location	M <sub>2</sub>			S <sub>2</sub>		
	Observed/Modelled Amplitude	Real Difference	Percentage Difference	Observed/Modelled Amplitude	Real Difference	Percentage Difference
Schooner Harbour	207.5/207.2	-0.3	-0.1	71.0/68.4	-2.6	-3.7
Port de Boucherville	144.4/143.9	-0.5	-0.3	53.9/54.0	0.1	0.2
Port de La Perriere	94.1/99.3	5.2	5.5	37.7/38.7	1.0	2.7
Digges Harbour	100.2/100.0	-0.2	-0.2	39.3/39.0	-0.3	-0.8
Sugluk	155.1/156.8	1.7	1.1	58.5/58.3	-0.2	-0.3
Deception Bay	171.7/171.7	0.0	0.0	60.3/61.1	0.8	1.3
Douglas Harbour	259.3/258.0	1.3	-0.5	92.0/81.5	-10.5	-11.4
Wakeham Bay	336.5/276.7	-59.8	-17.8	162.6/83.0	-79.6	-49.0
Doctor Island	257.5/271.0	13.5	5.2	87.4/80.6	-6.8	-7.8
Stupart Bay	274.9/275.0	0.1	0.0	92.9/82.3	-10.6	-11.4
Diana Bay	293.0/293.1	0.1	0.0	99.3/82.1	-17.2	-17.3
Koartac	266.5/292.6	26.1	9.8	91.8/82.5	-9.3	-10.1
Basking Island	316.6/349.7	33.1	10.5	99.9/99.1	-0.8	-0.8
Pikiyulik Island	304.8/349.7	44.9	14.7	94.7/98.4	3.7	3.9
Agvik Island	349.3/359.5	10.2	2.9	117.0/102.7	-14.3	-12.2
Hopes Advance Bay	388.3/388.2	-0.1	0.0	125.2/110.8	-14.4	-11.5
Leaf Basin	443.1/407.2	-35.9	-8.1	121.3/112.9	-8.4	-6.9
Koksoak River Entrance	408.7/417.7	9.0	2.2	135.9/113.7	-22.2	-16.3
Port Burwell	214.2/213.1	-1.1	-0.5	65.2/63.5	-1.7	-2.6
Williams Harbour	98.1/86.3	-11.8	-12.0	23.7/23.5	-0.2	-0.8
Acadia Cove	216.0/219.2	3.2	1.5	89.0/73.7	-15.3	-17.2
Breevort Harbour	180.7/180.7	0.0	0.0	64.0/64.0	0.0	0.0
Frobisher S. Farthest	329.5/324.8	-5.0	-1.4	110.4/105.0	-5.4	-4.9
Resor Island	334.3/352.2	18.0	5.4	118.8/115.4	-3.4	-2.9
Frobisher	345.2/356.5	11.3	3.3	117.4/115.6	-1.8	-1.5
Lake Harbour	349.6/353.2	3.6	1.0	119.9/116.7	-3.2	-2.7
Ashe Inlet	335.2/327.0	-8.2	-2.4	121.3/99.8	-21.5	-17.7
Ungava Bay	420.7/423.4	2.7	0.6	133.3/113.3	-20.0	-15.0

COMPARISON OF AMPLITUDES OF OBSERVED AND MODELLED TIDES (cm)

Location	N <sub>2</sub>			K <sub>1</sub>		
	Observed/Modelled Amplitude	Real Difference	Percentage Difference	Observed/Modelled Amplitude	Real Difference	Percentage Difference
Schooner Harbour	41.4/39.5	-1.9	-4.6	8.2/7.9	-0.3	-3.7
Port de Boucherville	27.4/27.0	-0.4	-1.5	6.7/6.6	-0.1	-1.5
Port de La Perriere	18.2/20.0	-1.8	-9.9	4.2/5.0	0.8	19.0
Digges Harbour	39.3/20.0	-19.3	-49.1	5.4/5.1	-0.3	-5.6
Sugluk	30.7/30.7	0.0	0.0	10.0/7.0	-3.0	-30.0
Deception Bay	34.3/35.3	1.0	2.9	8.3/7.6	-0.7	-8.4
Douglas Harbour	48.1/52.0	3.9	8.1	10.5/11.0	0.5	4.8
Wakeham Bay	69.6/55.6	-14.0	-20.1	13.4/12.0	-1.4	-10.4
Doctor Island	51.5/54.3	2.8	5.4	14.9/12.0	-2.9	-19.5
Stupart Bay	54.8/54.9	0.1	0.2	14.3/11.8	-2.5	-17.5
Diana Bay	58.6/58.5	-0.1	-0.2	15.7/14.0	-1.7	-10.8
Koartac	51.1/58.1	7.0	13.7	6.8/14.2	7.4	108.8
Basking Island	58.8/68.3	9.5	16.2	14.3/15.2	0.9	6.3
Pikiyulik Island	55.1/70.0	14.9	27.0	14.9/15.2	0.3	2.0
Agvik Island	64.6/68.3	3.7	5.7	17.6/15.6	-2.0	-11.4
Hopes Advance Bay	83.2/75.9	-7.3	-8.8	20.7/15.9	-4.8	-23.2
Leaf Basin	91.7/78.4	-13.3	-14.5	18.5/16.2	-2.3	-12.4
Koksoak River Entrance	75.8/75.9	0.1	0.1	15.8/16.0	0.2	1.3
Port Burwell	42.0/42.0	0.0	0.0	12.4/14.7	2.3	-18.5
Williams Harbour	30.1/21.5	-8.6	-28.6	19.2/15.4	-3.8	-19.8
Acadia Cove	43.0/44.0	1.0	2.3	13.0/15.2	2.2	16.9
Breevort Harbour	34.7/34.7	0.0	0.0	17.0/17.0	0.0	0.0
Frobisher S. Farthest	54.0/67.4	13.4	24.8	18.0/18.7	0.7	3.9
Resor Island	66.4/74.5	8.1	12.2	20.1/19.2	-0.9	-4.5
Frobisher	67.7/74.7	7.0	10.3	18.4/19.2	0.8	4.3
Lake Harbour	67.6/72.7	5.1	7.5	15.2/15.6	0.4	2.6
Ashe Inlet	67.0/66.9	-0.1	-0.1	15.8/14.3	-1.5	-9.5
Ungava Bay	-/79.1	-	-	17.7/16.1	-1.6	-9.0

COMPARISON OF PHASES OF OBSERVED AND MODELLED TIDES (degrees)

Location	M <sub>2</sub>			S <sub>2</sub>		
	Observed/Modelled Phase	Real Difference	Percentage Difference	Observed/Modelled Phase	Real Difference	Percentage Difference
Schooner Harbour	316.0/316.0	0.0	0.0	9.0/6.0	3.0	0.8
Port de Boucherville	270.0/270.0	0.0	0.0	326.0/326.0	0.0	0.0
Port de La Perriere	268.0/280.0	-12.0	-3.3	322.0/325.0	-3.0	-0.8
Digges Harbour	279.0/280.0	-1.0	-0.3	325.0/325.0	0.0	0.0
Sugluk	255.0/250.0	5.0	1.4	304.0/310.0	-6.0	-1.7
Deception Bay	248.2/246.0	2.2	0.6	304.0/306.0	-2.0	-0.6
Douglas Harbour	231.0/230.0	1.0	0.3	298.0/287.0	11.0	3.1
Wakeham Bay	234.0/226.0	8.0	2.2	279.1/282.0	-2.9	-0.8
Doctor Island	237.0/226.0	11.0	3.1	289.0/284.0	5.0	1.4
Stupart Bay	225.0/224.0	1.0	0.3	282.0/280.0	2.0	0.6
Diana Bay	224.2/218.0	6.2	1.7	275.5/269.0	6.5	1.8
Koartac	253.9/214.0	39.9	11.1	311.3/266.0	45.3	12.6
Basking Island	253.0/213.0	40.0	11.1	313.0/262.0	51.0	14.2
Pikiyulik Island	251.0/213.0	38.0	10.6	302.0/263.0	39.0	10.8
Agvik Island	225.0/214.0	11.0	3.1	275.0/264.0	11.0	3.1
Hopes Advance Bay	225.0/219.0	6.0	1.7	280.0/268.0	12.0	3.3
Leaf Basin	251.0/226.0	25.0	6.9	314.0/272.0	42.0	11.7
Koksoak River Entrance	229.0/228.0	1.0	0.3	282.0/284.0	-2.0	-0.6
Port Burwell	209.0/226.0	17.0	4.7	258.0/276.0	-18.0	-5.0
Williams Harbour	187.5/196.0	8.5	2.4	227.0/217.0	10.0	2.8
Acadia Cove	211.0/198.0	13.0	3.6	246.0/244.0	18.0	5.0
Breevort Harbour	157.0/157.0	0.0	0.0	195.0/195.0	0.0	0.0
Frobisher S. Farthest	218.5/182.0	36.5	10.1	267.1/223.0	44.1	12.3
Resor Island	197.0/183.0	14.0	3.9	242.0/226.0	16.0	4.4
Frobisher	193.1/184.0	9.1	2.5	238.8/226.0	12.8	3.6
Lake Harbour	231.7/224.0	7.7	2.1	280.9/289.0	-8.1	-2.3
Ashe Inlet	230.0/229.0	1.0	0.3	287.0/284.0	3.0	0.8
Ungava Bay	232.9/230.0	2.9	0.8	283.9/273.0	10.9	3.0

$$\text{Percentage Difference} = \frac{(\text{observed phase} - \text{modelled phase})}{360} \times 100\%$$

COMPARISON OF PHASES OF OBSERVED AND MODELLED TIDES (degrees)

Location	N <sub>2</sub>			K <sub>1</sub>		
	Observed/Modelled Phase	Real Difference	Percentage Difference	Observed/Modelled Phase	Real Difference	Percentage Difference
Schooner Harbour	289.6/288.0	1.6	0.4	147.0/145.0	2.0	0.6
Port de Boucherville	331.6/258.0	73.6	20.4	113.0/118.0	-5.0	-1.4
Port de La Perriere	332.6/252.0	806	22.4	102.1/104.0	-1.9	-0.5
Digges Harbour	251.6/252.0	-0.4	-0.1	104.0/104.0	0.0	0.0
Sugluk	227.6/235.0	-7.4	-2.1	90.0/ 94.0	-4.0	-1.1
Deception Bay	222.6/227.0	-4.4	-1.2	83.0/ 88.0	-5.0	-1.4
Douglas Harbour	214.6/214.0	0.6	0.2	60.0/ 90.0	-30.0	-8.3
Wakeham Bay	212.0/210.0	2.0	0.6	77.2/ 89.0	-11.8	-3.3
Doctor Island	310.6/210.0	100.0	27.8	118.0/88.0	30.0	8.3
Stupart Bay	331.6/209.0	122.6	34.1	99.0/ 87.0	12.0	3.3
Diana Bay	198.0/202.0	-4.0	-1.1	87.9/ 86.0	1.9	0.5
Koartac	226.2/199.0	27.2	7.6	122.1/86.0	36.1	10.0
Basking Island	235.0/198.0	37.0	10.3	112.0/86.0	26.0	7.2
Pikiyulik Island	224.0/194.0	30.0	8.3	105.0/86.0	19.0	5.3
Agvik Island	199.0/199.0	0.0	0.0	110.0/87.0	23.0	6.4
Hopes Advance Bay	188.0/204.0	-16.0	-4.4	97.0/ 89.0	8.0	2.2
Leaf Basin	253.0/209.0	44.0	12.2	113.0/91.0	22.0	6.1
Koksoak River Entrance	196.0/210.0	-14.0	-3.9	91.0/ 92.0	-1.0	-0.3
Port Burwell	177.6/204.0	-26.4	-7.3	90.0/ 94.0	-4.0	-1.1
Williams Harbour	154.4/185.0	-30.6	-8.5	72.5/76.0	-3.5	-1.0
Acadia Cove	- /170.0	-	-	115.0/87.0	28.0	7.5
Breevort Harbour	132.6/133.0	-0.4	0.1	49.0/49.0	0.0	0.0
Frobisher S. Farthest	188.6/164.0	24.6	6.8	100.6/79.0	21.6	6.0
Resor Island	168.6/166.0	2.6	0.7	96.0/80.0	16.0	4.4
Frobisher	164.7/166.0	-1.3	-0.4	85.5/80.0	5.5	1.5
Lake Harbour	204.4/220.0	-15.6	-4.3	102.1/102.0	0.1	0.0
Ashe Inlet	208.6/210.0	-1.4	-0.4	103.0/100.0	3.0	0.8
Ungava Bay	205.7/208.0	-2.3	-0.6	91.8/92.0	-0.2	-0.1

69

$$\text{Percentage Difference} = \frac{(\text{observed phase} - \text{modelled phase})}{360} \times 100\%$$